AD_____

Award Number: DAMD17-99-1-9361

TITLE: Selective DNA Delivery to Breast Cancer Cells

PRINCIPAL INVESTIGATOR: Stephen Dewhurst, Ph.D.

CONTRACTING ORGANIZATION: University of Rochester
Rochester, New York 14627

REPORT DATE: June 2003

TYPE OF REPORT: Final

PREPARED FOR: U.S. Army Medical Research and Materiel Command
Fort Detrick, Maryland 21702-5012

DISTRIBUTION STATEMENT: Approved for Public Release;
Distribution Unlimited

# REPORT DOCUMENTATION PAGE

*Form Approved*
*OMB No. 074-0188*



| 1. AGENCY USE ONLY (Leave blank) | 2. REPORT DATE | 3. REPORT TYPE AND DATES COVERED |
|---|---|---|
| | June 2003 | Final (1 Jun 1999 - 31 May 2003) |

**4. TITLE AND SUBTITLE**
Selective DNA Delivery Breast Cancer Cells

**5. FUNDING NUMBERS**
DAMD17-99-1-9361

**6. AUTHOR(S)**
Stephen Dewhurst, Ph.D.

**7. PERFORMING ORGANIZATION NAME(S) AND ADDRESS(ES)**
University of Rochester
Rochester, New York 14627

E-Mail: stephen_dewhurst@urmc.rochester.edu

**8. PERFORMING ORGANIZATION REPORT NUMBER**

**9. SPONSORING / MONITORING AGENCY NAME(S) AND ADDRESS(ES)**
U.S. Army Medical Research and Materiel Command
Fort Detrick, Maryland 21702-5012

**10. SPONSORING / MONITORING AGENCY REPORT NUMBER**

**11. SUPPLEMENTARY NOTES**

**12a. DISTRIBUTION / AVAILABILITY STATEMENT**
Approved for Public Release; Distribution Unlimited

**12b. DISTRIBUTION CODE**

**13. ABSTRACT (Maximum 200 Words)**

The hypothesis of this research was that specific cell-binding proteins or peptides could be used to enhance (therapeutic) DNA delivery to breast carcinomas. This hypothesis was experimentally tested, with the following results:

(1) Recombinant adenovirus type 7 penton base protein (Ad7PB) was shown to mediate DNA transfer into mammalian cells, when coupled to plasmid DNA via a bifunctional peptide linker. However, the efficiency of DNA transfer was poor.

(2) Since CD40 is highly expressed on some breast carcinomas, we selected for CD40-binding peptides using phage display technology. When coupled to the surface of adenovirus vectors, these peptides dramatically enhanced virally-mediated gene delivery to CD40-positive murine and human cells.

(3) Since $\alpha v\beta 3$ integrin is expressed in many breast carcinomas, we generated novel $\alpha v\beta 3$-binding proteins by the directed mutagenesis of a natural integrin-binding protein, the tenth fibronectin type III domain (FNfn10). A novel derivative of FNfn10 was identified and shown to bind with high affinity and specificity to purified $\alpha v\beta 3$ integrin. It also interacted with cell surface-expressed $\alpha v\beta 3$, as determined by flow cytometry, but did not bind detectably to other cell surface integrins.

**Overall**, these experiments have provided important tools and insights that will enhance gene transfer to breast carcinomas.

**14. SUBJECT TERMS**
Breast cancer, her2, adenovirus, phage display, gene transfer

**15. NUMBER OF PAGES**
39

**16. PRICE CODE**

| 17. SECURITY CLASSIFICATION OF REPORT | 18. SECURITY CLASSIFICATION OF THIS PAGE | 19. SECURITY CLASSIFICATION OF ABSTRACT | 20. LIMITATION OF ABSTRACT |
|---|---|---|---|
| Unclassified | Unclassified | Unclassified | Unlimited |

## FOREWORD

Opinions, interpretations, conclusions and recommendations are those of the author and are not necessarily endorsed by the U.S. Army.

N/A Where copyrighted material is quoted, permission has been obtained to use such material.

N/A Where material from documents designated for limited distribution is quoted, permission has been obtained to use the material.

X Citations of commercial organizations and trade names in this report do not constitute an official Department of Army endorsement or approval of the products or services of these organizations.

X In conducting research using animals, the investigator(s) adhered to the "Guide for the Care and Use of Laboratory Animals," prepared by the Committee on Care and use of Laboratory Animals of the Institute of Laboratory Resources, national Research Council (NIH Publication No. 86-23, Revised 1985).

X For the protection of human subjects, the investigator(s) adhered to policies of applicable Federal Law 45 CFR 46.

In conducting research utilizing recombinant DNA technology, the investigator(s) adhered to current guidelines promulgated by the National Institutes of Health.

In the conduct of research utilizing recombinant DNA, the investigator(s) adhered to the NIH Guidelines for Research Involving Recombinant DNA Molecules.

N/A In the conduct of research involving hazardous organisms, the investigator(s) adhered to the CDC-NIH Guide for Biosafety in Microbiological and Biomedical Laboratories.

PI - Signature 5/21/03 Date

## Table of Contents

## INTRODUCTION

A number of gene delivery systems, including virally-based vectors as well as non-viral methods, are presently being explored as potential DNA delivery vehicles for gene- and immuno-therapy of breast cancer. However, currently available DNA delivery vehicles for gene therapy of breast cancer have a very wide host cell range, making it difficult to specifically target them to tumor cells. Therefore, the experiments that were performed under the auspices of this grant award were aimed at developing innovative new approaches that will allow one to selectively target DNA molecules to breast cancer cells. The underlying hypothesis which we explored was as follows: that one can use specific protein or peptide sequences to selectively target linked DNA molecules to breast cancer cells. This hypothesis was explored by a combination of approaches, including the use of peptide phage display libraries and recombinant adenovirus-derived gene delivery systems.

## BODY

Approved Tasks

The following tasks were outlined in the approved statement of work for this grant:

- *Task 1.* Analysis of DNA delivery by adenovirus penton base proteins (AdPB) (months 1 - 12)
- *Task 2.* Application of phage display technology to the identification of breast cancer targeting peptides (months 1 - 15). *Timeline extended to 1-36 months.*
- *Task 3.* Analysis of DNA delivery to breast cancer cells by novel peptides (months 16-30). *Timeline extended to 16-36 months.*
- *Task 4.* Studies of DNA delivery using an *in vivo* xenograft model for breast cancer (months 25-36). *Originally included in the approved tasks, but ultimately deferred until a future date, when more compelling in vitro data exist. The adenovirus penton base proteins developed in Aim 1 did not show sufficient promise to merit performance of these in vivo studies. This decision was made for two major reasons. First, the AdPB proteins mediated DNA delivery with a lower level of efficiency than commercially available reagents such as lipofectamine. Second, DNA delivery by AdPB required the formation of unstable trimolecular complexes, incorporating AdPB, DNA and a bridging peptide. It was deemed highly unlikely that a tirmolecular complex of this kind, held together by low-affinity peptide-DNA and peptide-protein interactions would remain intact in vivo We therefore decided to extend Task 2, because we obtained exciting preliminary data in these experiments. In particular, we focussed our attention on the derivation of more promising lead molecules, with the ability to interact with key cell surface receptors expressed on breast cancers (i.e., $\alpha v\beta 3$ integrin and CD40; see below).*

Research Accomplishments associated with the above tasks

***Task 1:*** Experiments on the analysis of DNA delivery by adenovirus penton base proteins are summarized in the paper by Bal et al (Appendix), which was published in Eur. J. Biochem (Bal *et al.*). Key findings, reported in this paper, were as follows:

- Full length Ad7 penton base protein (Ad7PB) and short peptides corresponding to the integrin-binding domain from Ad7PB (Ad7PB-derived RGD peptides) were capable of mediating DNA transfer into 293 cells. However, the efficiency of this DNA transfection was approximately 100-1000x worse than that mediated by standard methods (lipofectamine).

- Ad7PB and Ad7PB-derived RGD peptides gave a very low (undetectable) rate of DNA transfer into primary cells (including dendritic cells) and were also highly inefficient in mediated DNA transfer into cell lines other than 293 cells.

- Ad7PB-mediated DNA transfer was highly variable

While encouraging, our findings with the Ad7PB DNA delivery method suggested to us that his approach is highly unlikely to prove suitable for *in vivo* DNA delivery. This obligated us to explore further approaches to the generation of cell-targeting approaches and to extend the timeline for Task 2. Ultimately, this resulted in a decision to forgo Task 4, so as to focus on the generation of useful reagents capable of most effectively targeting breast cancer cells. Future experiments (supported by new grant applications) will be conducted to pursue the effectiveness of these DNA delivery methods, with respect to gene transfer into breast cancer cells.

***Task 2:*** Experiments aimed at the identification of novel breast cancer targeting peptides generated results that included the following findings (which were previously reported in the year one and year two annual reports for this award):

- Construction of a random peptide display library in T7 bacteriophage
- Development of protocols to enrich for phage populations capable either of binding to specific cellular receptors (CD40, $\alpha_v\beta_3$ integrin), or capable of undergoing internalization in cultured human cells
- Application of these methods to breast cancer cells, and recovery of phage populations with an enhanced ability to enter breast cancer cells
- Application of these methods to specific endocytosing cell surface receptos expressed on breast cancer cells (CD40, $\alpha_v\beta_3$), and recovery of phage populations with an enhanced ability to bind to these molecules
- Retargeting of adenovirus vectors using phage-selected peptides. In these experiments we have elected to explore the feasibility of using phage-selected peptides to retarget adenovirus vectors to the CD40 molecule, since this receptor is highly expressed on some breast carcinomas (6, 10). In pilot feasibility experiments, we have examined ability of our CD40-selected peptides to enhance adenovirus-mediated gene transfer into primary human and murine dendritic cells (DC), which express CD40 and which also express very low levels of the

primary adenovirus receptor (the coxsackie and adenovirus receptor, or CAR). These pilot experiments were approached by synthesizing bifunctional oligopeptides, containing two distinct domains, separated by a short spacer (GGGS). Functional peptide domains were as follows: (1) a motif that binds to the adenovirus fiber protein (MH20; RAIVGFRVQWLRRYFVNGSR), and (2) a phage-derived peptide selected for the ability to bind to CD40 (ATYSEFPGNLKP) or a mutated derivative of the same peptide in which the consensus CD40-binding region was replaced by alanines (ATYSEAAAALKP). The peptides were then added to a fixed amount of an adenovirus vector expressing the jellyfish green fluorescent protein (Ad:GFP). The peptide-conjugated virus preparation was then added to the target cells, and GFP expression was quantitated 48 hours later, using flow cytometry. The results of this experiment revealed that phage-selected peptides can indeed enhance adenovirus infection of CD40+ dendritic cells (both human and murine).

**New findings**, derived from the third and final project year, are summarized below and in greater detail in the manuscript by Richards and coworkers (see Appendix; *Richards J., et al*).

Background: Why Target αvβ3?

Alphavbeta3 (CD51/CD61) is a member of the integrin family of cell surface adhesion receptors. Over 20 different αβ integrin heterodimers exist, each with different tissue and ligand specifities. Normal tissue distribution of αvβ3 is generally limited to high levels of expression on osteoclasts, with lower levels observed on platelets, megakaryocytes, kidney, vascular smooth muscle, placenta, dendritic cells, and in varying amounts on normal endothelium.

αvβ3 integrin is a multifunctional cell surface receptor that has pleiotropic roles in normal cell growth and survival, and which can contribute to oncogenesis. Consistent with this, upregulation of αvβ3 expression has been observed on the endothelial cells of angiogenic vessels, and binding of αvβ3 to the basement membrane is a critical step in the angiogenesis induced by basic fibroblast growth factor and tumor necrosis factor alpha (5). Expression of αvβ3 has also been implicated in tumor invasion, and it has been shown that αvβ3 binds matrix metalloproteinase-2 (MMP-2) and presents MMP-2 on the surface of invasive carcinomas and on invasive angiogenic endothelial cells (2, 8).

αvβ3 also regulates cell growth and survival, since ligation of this receptor can, under some circumstances, induce apoptosis in tumor cells (7). Furthermore, disruption of cell adhesion with anti-αvβ3 antibodies, RGD peptides, and other integrin antagonists has been shown to slow tumor growth (1, 3, 4). Finally, the selective upregulation of αvβ3 expression on tumor blood vessels is also being explored as the basis for imaging of neoplastic lesiosn, and the αvβ3-specific antibody LM609 has been successfully used for this purpose *in vivo* (9).

Novel molecules capable of binding with high specificity to αvβ3 integrin have potential utility in several applications, and as a consequence, αvβ3 is an important target for drug discovery and selection of new binding ligands. The tenth fibronectin type III domain (FNfn10) was developed as a phage display scaffold because of its small size (94 residues), monomeric assembly, and ability to retain its folded β-sheet morphology while exposed loops were randomized. In addition, FNfn10 lacks cysteine residues and requires no post-translational modification, allowing for large-scale bacterial expression. We reasoned that since FNfn10 binds αvβ3 *in vivo*, affinity maturation of the RGD sequence in the exposed FG loop might result in a modified FNfn10 with high-affinity for αvβ3. We further reasoned that a modified derivative of FNfn10 might be particulatly useful for vector or gene delivery applications because of (1) the small size of this protein, (2) its simple

monomeric structure, and (3) its lack of disulfide bonds. These considerations suggested to us that it ought to be possible to place a modified FNfn10 on the surface of bacteriophage or virus vectors (for DNA delivery applications) and also to derivatize the protein in such a way as to link it directly to plasmid DNA molecules. As such, the modified FNfn10 protein might be expected to have major advantages over the adenovirus penton base protein (AdPB), which emerged as a somewhat more difficult reagent, due in part to its larger size, disulfide bonds and propensity to form multimers.

Summary of findings

As noted above, we have utilized a natural integrin-binding protein, the tenth fibronectin type III domain (FNfn10), as a scaffold for the selection of novel $\alpha v\beta 3$-binding molecules. By randomizing residues surrounding the RGD sequence in the flexible FG loop of FNfn10, we selected $\alpha v\beta 3$-binding modified FNfn10 clones with a novel RGDWXE consensus sequence. One of these clones, 3JCLI4-FNfn10, binds with high affinity and specificity to purified $\alpha v\beta 3$ integrin. It also interacts with cell surface-expressed $\alpha v\beta 3$, as determined by flow cytometry, but does not bind detectably to other cell surface integrins. Taken together, these data show that 3JCL14-FNfn10 is a specific, high-affinity $\alpha v\beta 3$-binding protein which may have utility in future applications involving the targeting of $\alpha v\beta 3$-positive cells.

**The complete results from this work are included in the Appendix, in the manuscript by Richards et al.**

## KEY RESEARCH ACCOMPLISHMENTS OF THIS WORK

- Recombinant, bacterially-expressed adenovirus type 7 penton base protein (Ad7PB) was shown to be capable of mediating DNA transfer into mammalian cells, when coupled to plasmid DNA via a bifunctional peptide linker. However, the efficiency of this DNA transfection was rather variable and in general, considerably inferior to that mediated by standard methods (lipofectamine) in cell lines and primary cells.

- Construction of a random peptide display library in T7 bacteriophage, and use of this library to select for phage populations capable of binding to specific cellular receptors, including a key integrin receptor that is expressed on some breast cancers and on breast tumor vasculature ($\alpha_v\beta_3$ integrin) and a second receptor that is also expressed on some breast carcinomas (CD40).

- Successful retargeting of adenovirus vectors using phage-selected peptides. In these experiments we used phage-selected, CD40-binding peptides to show that one can substantially enhance the efficiency with which adenovirus vectors deliver DNA to cells which express CD40, and which also express only very low levels of the major adenovirus receptor (the coxsackie-and-adenovirus receptor, or CAR).

- Utilization of a natural integrin-binding protein, the tenth fibronectin type III domain (FNfn10), as a scaffold for the selection of novel $\alpha v\beta 3$-binding molecules and successfiul identification of novel integrin-binding proteins using this method. Briefly, by randomizing residues surrounding the RGD sequence in the flexible FG loop of FNfn10, we selected $\alpha v\beta 3$-binding modified FNfn10 clones with a novel RGDWXE consensus sequence. One of these clones, 3JCLI4-FNfn10, binds with high affinity and specificity to purified $\alpha v\beta 3$ integrin. It also interacts with cell surface-expressed $\alpha v\beta 3$, as determined by flow cytometry, but does not bind detectably to other cell surface integrins. Taken together, these data show that 3JCL14-FNfn10 is a specific, high-affinity $\alpha v\beta 3$-binding protein. These properties, combined with the small, monomeric, cysteine-free and highly stable structure of 3JCLI4-FNfn10, may make this protein useful in future applications involving the targeting of $\alpha v\beta 3$-positive cells.

## REPORTABLE OUTCOMES

**Manuscripts, abstracts, presentations:** See Bibliography

**Patents and licenses applied for and/or issued:** None

**Degrees obtained that are supported by this award:** None

**Development of cell lines, tissue or serum repositories:** None

**Informatics such as databases and animal models, etc:** None

**Funding applied for based on work supported by this award:** None

**Employment or research opportunities applied for and/or received on experiences/training supported by this award:** Research training was provided for Ms. Michelle Miller was provided (Ms. Miller is a 1999 college graduate, who has been working on this project as a laboratory technician). Ms. Miller is presently working on her M.S. in Microbiology and Immunology, a goal which has been facilitated by her training on this research project. Research training for two summer undergraduate researchers, Ms. Johanna Abend and Ms. Laura McLane, was also provided. Ms. Abend's entered the graduate (Ph.D.) program in summer of 2003 – a goal which was enhanced by her training under this award. Ms. McLane's long-term goals are similar, although she is presently employed as a laboratory technician at Emory University.

## CONCLUSIONS

The conclusions which can be drawn from this research are as follows:

- Recombinant, bacterially-expressed adenovirus type 7 penton base protein (Ad7PB) can be used to mediate DNA transfer into mammalian cells, when it is coupled to plasmid DNA via a bifunctional peptide linker. However, the efficiency of this DNA transfection is variable and it is, in general, much less efficient than standard methods for plasmid DNA transfer into mammalian cells.

- Adenovirus vectors can be successfully targeted to specific cell types of interest, using specific ligand-binding peptides that can be identified through the application of phage display technology. In particular, we were able to show that bifunctional CD40-binding peptides can be used to enhance adenovirus infection of CD40-positive murine and human cells which are deficient in the primary adenovirus receptor (the coxsackie-and-adenovirus receptor, or CAR). Since many breast carcinomas express high levels of CD40 and are deficient in CAR, these results are directly relevant to improving gene delivery to breast cancer cells.

- A natural integrin-binding protein, the tenth fibronectin type III domain (FNfn10), can be successfully used as a scaffold for the selection of novel $\alpha v\beta 3$-binding molecules. By randomizing residues surrounding the RGD sequence in the flexible FG loop of FNfn10, we selected $\alpha v\beta 3$-binding modified FNfn10 clones with a novel RGDWXE consensus sequence. One of these clones, 3JCLI4-FNfn10, was shown to bind with high affinity and specificity to purified $\alpha v\beta 3$ integrin. It also interacted with cell surface-expressed $\alpha v\beta 3$, as determined by flow cytometry, but did not bind detectably to other cell surface integrins. Thus, we were able to derive a novel, specific, high-affinity $\alpha v\beta 3$-binding protein. This protein is small, monomeric, cysteine-free and highly stable, which may make it very useful in future applications involving the targeting or detection of $\alpha v\beta 3$-positive cells (such as those found in breast tumor vasculature).

### "So What Section"

The knowledge gained from these experiments advances the basic goals proposed in the original grant application, and provides important tools and insights into approaches which can be used to selectively deliver therapeutic DNA to breast cancers.

# REFERENCES


1. **Brooks, P. C., S. Stromblad, R. Klemke, D. Visscher, F. H. Sarkar, and D. A. Cheresh.** 1995. Antiintegrin alpha v beta 3 blocks human breast cancer growth and angiogenesis in human skin. J Clin Invest **96:**1815-22.
2. **Brooks, P. C., S. Stromblad, L. C. Sanders, T. L. von Schalscha, R. T. Aimes, W. G. Stetler-Stevenson, J. P. Quigley, and D. A. Cheresh.** 1996. Localization of matrix metalloproteinase MMP-2 to the surface of invasive cells by interaction with integrin alpha v beta 3. Cell **85:**683-93.
3. **Chatterjee, S., K. H. Brite, and A. Matsumura.** 2001. Induction of apoptosis of integrin-expressing human prostate cancer cells by cyclic Arg-Gly-Asp peptides. Clin Cancer Res **7:**3006-11.
4. **Chatterjee, S., A. Matsumura, J. Schradermeier, and G. Y. Gillespie.** 2000. Human malignant glioma therapy using anti-alpha(v)beta3 integrin agents. J Neurooncol **46:**135-44.
5. **Friedlander, M., P. C. Brooks, R. W. Shaffer, C. M. Kincaid, J. A. Varner, and D. A. Cheresh.** 1995. Definition of two angiogenic pathways by distinct alpha v integrins. Science **270:**1500-2.
6. **Hirano, A., D. L. Longo, D. D. Taub, D. K. Ferris, L. S. Young, A. G. Eliopoulos, A. Agathanggelou, N. Cullen, J. Macartney, W. C. Fanslow, and W. J. Murphy.** 1999. Inhibition of human breast carcinoma growth by a soluble recombinant human CD40 ligand. Blood **93:**2999-3007.
7. **Kozlova, N. I., G. E. Morozevich, A. N. Chubukina, and A. E. Berman.** 2001. Integrin alphavbeta3 promotes anchorage-dependent apoptosis in human intestinal carcinoma cells. Oncogene **20:**4710-7.
8. **Silletti, S., T. Kessler, J. Goldberg, D. L. Boger, and D. A. Cheresh.** 2001. Disruption of matrix metalloproteinase 2 binding to integrin alpha vbeta 3 by an organic molecule inhibits angiogenesis and tumor growth in vivo. Proc Natl Acad Sci U S A **98:**119-24.
9. **Sipkins, D. A., D. A. Cheresh, M. R. Kazemi, L. M. Nevin, M. D. Bednarski, and K. C. Li.** 1998. Detection of tumor angiogenesis in vivo by alphaVbeta3-targeted magnetic resonance imaging. Nat Med **4:**623-6.
10. **Tong, A. W., M. H. Papayoti, G. Netto, D. T. Armstrong, G. Ordonez, J. M. Lawson, and M. J. Stone.** 2001. Growth-inhibitory effects of CD40 ligand (CD154) and its endogenous expression in human breast cancer. Clin Cancer Res **7:**691-703.

## BIBLIOGRAPHY (PUBLICATIONS)

*These materials are all also included as Appendices*

**Manuscripts:**

H. P. Bal, J. Chroboczek, G. Schoehn, R.W.H. Ruigrok, S. Dewhurst. Adenovirus type 7 penton: Purification of soluble pentamers from *E. coli* and development of an integrin-dependent gene delivery system. **Eur. J. Biochem.** 267:6074-6081, 2000.

Richards, J., Miller, M., Abend, J., Koide, A., Koide, S., and Dewhurst, S. Engineered fibronectin type III domain with a RGDWXE sequence binds with enhanced affinity and specificity to human αvβ3 integrin. **J. Mol. Biol.** 326:1475-1488, 2003.

**Abstracts:**

H.P. Bal, J. Chroboczek, R.W.H. Ruigrok, S. Dewhurst. Adenovirus type 7 penton: Purification of soluble pentamers from *E. coli* and development of an integrin-dependent gene delivery system. Presented at: Third Annual Meeting of the American Society of Gene Therapy, May 31 - June 4, 2000 (Denver, Colorado).

J. Richards, M. Miller, A. Koide, S. Koide, S. Dewhurst. Directed evolution of fibronectin type III domain toward high affinity molecules binding to $\alpha_v\beta_3$ integrin. Presented at: "Phage Display Technologies: Directed Protein Evolution": April 2001, Boston, Mass.

## LIST OF PERSONNEL

*List of personnel who were supported from the research effort*

| **Individual** | **Role** |
|---|---|
| Stephen Dewhurst, PhD | PI |
| John Frelinger, Ph.D. | CoPI (following departure of Dr. Challita-Eid) |
| Pia Challita-Eid, Ph.D. | CoPI (until her departure from UR, in 2000) |
| Michelle Miller, B.S. | Technician (2000-2002) |
| Laura McLane, B.S. | Summer undergraduate researcher (2000) |
| Johanna Abend, B.S. | Summer undergraduate researcher (2001) |
| Shikha Chakraborty-Sett, M.S. | Technician (prior to hiring of Ms. Miller, in 2000) |

# APPENDIX MATERIALS

| | |
|---|---|
| Award Number: | DAMD17-99-1-9361 |
| TITLE: | Selective DNA Delivery to Breast Cancer Cells |
| PRINCIPAL INVESTIGATOR: | Stephen Dewhurst, Ph.D. |
| CONTRACTING ORGANIZATION: | University of Rochester Medical Center<br>Rochester, New York 14642 |
| REPORT DATE: | June 2003 |
| TYPE OF REPORT: | Final |

## List of Materials Appended

**Manuscripts:**

H. P. Bal, J. Chroboczek, G. Schoehn, R.W.H. Ruigrok, S. Dewhurst. Adenovirus type 7 penton: Purification of soluble pentamers from *E. coli* and development of an integrin-dependent gene delivery system. Eur. J. Biochem. 267:6074-6081, 2000.

- 8 pages

Richards, J., Miller, M., Abend, J., Koide, A., Koide, S., and Dewhurst, S. Engineered fibronectin type III domain with a RGDWXE sequence binds with enhanced affinity and specificity to human αvβ3 integrin. **J. Mol. Biol.** 326:1475-1488, 2003.

- 14 pages

**Abstracts:**

H.P. Bal, J. Chroboczek, R.W.H. Ruigrok, S. Dewhurst. Adenovirus type 7 penton: Purification of soluble pentamers from *E. coli* and development of an integrin-dependent gene delivery system. Presented at: Third Annual Meeting of the American Society of Gene Therapy, May 31 - June 4, 2000 (Denver, Colorado).

- 1 page

J. Richards, M. Miller, A. Koide, S. Koide, S. Dewhurst. Directed evolution of fibronectin type III domain toward high affinity molecules binding to $\alpha_v\beta_3$ integrin. Presented at: "Phage Display Technologies: Directed Protein Evolution": April 2001, Boston, Mass.

- 1 page

## ABSTRACT #1

H. P. Bal, J. Chroboczek, R.W.H. Ruigrok, S. Dewhurst. Adenovirus type 7 penton: Purification of soluble pentamers from *E. coli* and development of an integrin-dependent gene delivery system. Oral Presentation at the Third Annual Meeting of the American Society of Gene Therapy, May 31 - June 4, 2000 (Denver, Colorado).

Adenoviral gene therapy vectors suffer from the disadvantages of toxicity and immunogenicity associated with the expression of adenoviral gene products from the vector backbone. We report here an alternate strategy for gene delivery that utilizes a single component of the adenoviral type 7 capsid - the penton (Ad 7 PB). The Ad7 PB gene was sequenced and its amino acid composition was deduced from its nucleotide sequence. Ad7 PB exhibited strict conservation of residues essential for pentamerization and fiber-binding. The penton was expressed in E. coli in the soluble form as a C-terminal fusion with GST (GST-Ad7 PB) and was purified by a single-step affinity chromatography. Both GST-Ad7 PB and cleaved (GST-free) Ad7 PB retained the ability to fold into native pentamers as observed by electron microscopy. GST-Ad7 PB was able to bind a synthetic peptide (FK20) derived from the Ad type 7 fiber and retard DNA through a polylysine chain present at the C-terminus of the linker peptide. GST-Ad7 PB was an effective cell transfecting agent when assayed on 293 cells. Transfection was not dependent upon the presence of lysosomotropic agents indicating efficient endosome escape capability. Excess of an RGD-containing peptide derived from Ad7 PB was able to inhibit transfection indicating specific integrin-mediated uptake of the GST-Ad7 PB-FK20-DNA complexe. Integrins have distinct cell-surface expression profiles that can be exploited for delivery to a variety of cell types of lymphoid, hematopoietic, endothelial and epithelial origin, in a specific manner. We propose that Ad7 pentons can be developed into powerful integrin-specific gene delivery agents.

## ABSTRACT #2

J. Richards, M. Miller, A. Koide, S. Koide, S. Dewhurst. Directed evolution of fibronectin type III domain toward high affinity molecules binding to $\alpha_v\beta_3$ integrin. Presented at: "Phage Display Technologies: Directed Protein Evolution": April 2001, Boston, Mass.

To improve the safety and efficacy of viral vectors in vaccine and gene therapy studies, it is advantageous to exercise control over the target cell tropism of the vectors. Since phage display technology allows for the selection of receptor-specific ligands, this technique has been adapted to screening for ligands to alpha$_v$beta$_3$ integrin. Our goal is to find both high-affinity binding ligands as well as ligands which will trigger receptor internalization. The cell adhesion receptor alpha$_v$beta$_3$ ($\alpha_v\beta_3$) integrin is a target of interest because of its expression on endothelial, dendritic, and cancer cells; its role in angiogenesis; and its involvement in the entry of many viruses (including adenovirus) into host cells. Previous work using phage display methods has resulted in the identification of short $\alpha_v\beta_3$-binding peptides containing the RGD consensus motif. However, we believe that it may be possible to select for higher affinity interactions using a small protein scaffold. Fibronectin is a natural ligand for $\alpha_v\beta_3$, which is compromised of multiple domains. The tenth fibronectin type III domain (FN3) of human fibronectin is a very stable, small (< 100 amino acids), structurally defined molecule with an immunoglobulin-like structure and a loop containing the RGD sequence. We have established phage display systems for FN3 [Koide et al. (1998) J. Mol. Biol. 284:1141]. By randomizing the residues in the FG loop of FN3 in a library displayed on M13 bacteriophage, sequences binding with much higher affinity to $\alpha_v\beta_3$ were selected, all of which contain a consensus sequence. This FN3 library has also been screened for internalization into selected cell lines of interest. Future applications may include not only gene therapy/vector development but also tumor inhibition and tumor detection/visualization.

*Eur. J. Biochem.* **267**, 6074–6081 (2000) © FEBS 2000

# Adenovirus type 7 penton

## Purification of soluble pentamers from *Escherichia coli* and development of an integrin-dependent gene delivery system

**Harshawardhan P. Bal[1,*], Jadwiga Chroboczek[2], Guy Schoehn[3], Rob W. H. Ruigrok[3] and Stephen Dewhurst[1,4]**

[1]*Department of Microbiology and Immunology, University of Rochester Medical Center, NY, USA;* [2]*Institut de Biologie Structurale, Grenoble, France;* [3]*European Molecular Biology Laboratory, Grenoble Outstation, France;* [4]*Cancer Center, University of Rochester, NY, USA*

Adenoviral gene therapy vectors suffer from the disadvantages of toxicity and immunogenicity associated with the expression of adenoviral genes from the vector backbone. We report here an alternative strategy for gene delivery that utilizes a single component of the adenoviral type 7 capsid, the penton base (Ad7PB). The *Ad7PB* gene was sequenced and its amino-acid composition was deduced from its nucleotide sequence. The penton was expressed in *Escherichia coli* as a soluble C-terminal fusion with glutathione S-transferase (GST–Ad7PB) and was purified by single-step affinity chromatography. Both GST–Ad7PB and cleaved (GST-free) Ad7PB retained the ability to fold into pentamers as observed by electron microscopy. GST–Ad7PB was able to bind a synthetic peptide (FK20) derived from the Ad type 7 fiber and retard DNA through a polylysine chain present at the C-terminus of this linker peptide. GST–Ad7PB was an effective cell transfecting agent when assayed on 293 cells. Transfection was not dependent upon the presence of lysosomotropic agents indicating efficient endosome escape capability. Excess of an RGD-containing peptide derived from Ad7PB was able to inhibit transfection indicating specific integrin-mediated uptake of the GST–Ad7PB–FK20–DNA complexes. We propose that Ad7 pentons can be developed into integrin-specific gene delivery agents.

*Keywords*: adenovirus; penton base; expression; integrin; gene delivery.

The initial interaction of adenovirus (Ad) with its host cell is orchestrated by a complex of two oligomeric viral capsid proteins, penton base (PB) and fiber, which together constitute the adenoviral penton. PB protein, present at each of the 12 vertices of the icosahedral Ad capsid, associates with the N-terminal tail portion of the fiber [1,2] while the C-terminal knob of the fiber, containing the cell-binding domain, projects away from the capsid. During the process of internalization, the Ad fiber first binds to a 46-kDa transmembrane protein that functions as a high-affinity receptor for a number of adenovirus subgroups and the coxsackie B viruses [3–5]. Ad internalization then proceeds via interaction of an arginine-glycine-aspartate (RGD) sequence on the Ad PB protein with $\alpha_v$ integrins on the cell surface; this interaction promotes virus-receptor endocytosis [6–13]. Human adenoviruses, probably with the exception of enteric serotypes, use the vitronectin binding integrins $\alpha_v\beta_3$ and $\alpha_v\beta_5$ to promote virus internalization [6,8].

Penton base monomeric polypeptide chains assemble in a fiber-independent manner into ≈300 kDa homopentamers. Penton bases of some serotypes can also form higher order structures, called dodecahedra, by a combination of 12 pentamers. Penton base dodecahedra are macromolecular complexes with a molecular mass of ≈3600 kDa. Both penton bases and dodecahedra have been shown to interact with cell-surface integrins via RGD motifs [6,8,14,15], which suggests that they might be capable of mediating internalization in the absence of fiber.

Nonviral gene delivery methods based on the native Ad cellular uptake machinery constitute an attractive alternative strategy to Ad vector-based methods. Ad PB does not influence cellular DNA or protein synthesis when added to cell cultures [8] and may therefore minimize both the immunogenicity and toxicity problems associated with the use of Ad vectors [16–18]. The development of an integrin-specific gene delivery method may constitute a powerful means for targeting a number of vital body tissues with applications in molecular medicine.

Integrins, a superfamily of α/β heterodimeric cell surface adhesion receptors, are known to mediate cell-cell adhesion and intracellular signaling events that regulate cell survival, proliferation, and migration [19]. Endothelial cells exposed to growth factors, or those undergoing angiogenesis in tumors, wounds, or inflammatory tissue, express high levels of $\alpha_v\beta_3$ integrins [20,21]. Brooks *et al* [22]. also demonstrated a significant role for $\alpha_v\beta_3$ integrins in human angiogenesis and breast tumor growth. For most integrins, the mechanism of ligand recognition depends on one of two short peptide motifs: RGD and leucine-aspartate-valine (LDV) [23,24], both of which are present in PBs from a number of Ad serotypes, including members of the subgroup B adenoviruses (Ad3, 7 and 11).

We have previously demonstrated that dodecahedra from Ad serotype 3 can be used for gene delivery [15]. In this strategy, a linker peptide containing the first 20 amino acids of Ad3 fiber was used to combine the cell-targeting activity of the Ad3 dodecahedron with a reporter plasmid construct to

*Correspondence to* S. Dewhurst, Department of Microbiology and Immunology, University of Rochester Medical Center, 575 Elmwood Avenue, Room 5-8106 (Box 672), Rochester, NY 14642, USA.
Fax: + 1 716 473 2361, Tel.: + 1 716 275 3216,
E-mail: stephen_dewhurst@urmc.rochester.edu

*Abbreviations*: Ad, Adenovirus; PB, penton base; Ad7PB, adenovirus type 7 penton base, GST, glutathione S-transferase; DMEM, Dulbecco's modified Eagle's medium; RLU, relative light units.

*Present address*: Cold Spring Harbor Laboratory, 1 Bungtown Road, Hershey, New York, NY 11724, USA.

(Received 15 May 2000, revised 2 August 2000, accepted 3 August 2000)

achieve intracellular delivery and expression of the reporter gene. The ternary dodecahedron-linker-DNA complex was demonstrated to enter target cells bearing integrin receptors.

Virus-cell interaction mediated through PB is known to vary by serotype [6,8,14,25]. Ad PBs show a high degree of diversity in the amino-acid sequence flanking the functionally relevant RGD tripeptide and it is possible that relative efficiencies of adenovirus PBs in mediating internalization may be a function of these differences. Ad serotype 7, another member of subgroup B adenoviruses, is known to form penton dodecahedra [26]. We therefore set out to sequence the PB gene from Ad serotype 7. Bacterial expression systems have previously been used for the expression and purification of PB from Ad serotype 2 and 12 [6,14]. However, both Ad2 PB and Ad12 PB were found to localize in *E. coli* as insoluble inclusion bodies. Our objective in pursuing this work was twofold: (a) to devise a simpler expression strategy for PB that yielded soluble protein and preserved the structural and functional integrity of the PB; and (b) to test the suitability of Ad7 penton as a gene transfer vehicle.

We describe here the sequencing, production from *E. coli* and the structural characterization of Ad7PB. The amino-acid composition of Ad7PB revealed strict conservation of functionally important residues. These included the essential integrin binding sites (RGD and LDV) and residues involved in pentamerization and stable fiber-PB binding. Ad7PB was expressed as a fusion with *Schistosoma japonicum* glutathione S-transferase (GST) and was purified in a soluble form from *E. coli*. The fusion protein (GST–Ad7PB) and the cleaved (GST-free) Ad7PB both retained their ability to pentamerize as shown by electron microscopy. Although dodecahedra were not detected in the preparation, GST-Ad7 PB proved to be an effective and integrin-specific cell transfecting agent.

## MATERIALS AND METHODS

### Sequencing of *Ad7PB* gene

DNA coding for Ad7PB was amplified by PCR using total Ad7 viral DNA as template. PCR primers were designed on the basis of homology with Ad3PB and had the following sequence: Ad31 forward primer: AGCGGATCCAGTACGATGAGGAGACGAGCCGTG; Ad32 reverse primer, AGCAAGCTTTTAGAAAGTGCGGCTTGAAAGAA. The *Ad7PB* gene was cloned into pFastBac1 (Life Technologies, Bethesda, MD, USA) as a *Bam*HI–*Hin*dIII fragment to produce pAd7PB-FastBac1. The *Ad7PB* gene in pAd7PB-FastBac1 was subsequently sequenced by automated procedures.

### Construction of expression plasmid pGST–Ad7PB

The *Ad7PB* gene was amplified by PCR from pAd7PB-FastBac1 and cloned as a *Bam*HI–*Eco*RI fragment in pGEX3X (glutathione S-transferase Gene Fusion system, Pharmacia). pGEX3X contains a factor Xa cleavage site between GST and PB to release GST and aid purification of the fusion partner. The primers used were: 7GX3UP forward primer: CTATGCGGGATCCCCATGAGGAGACGAGCCGTGCTA and 7GX3DN reverse primer: TGCTGCGAATTCTTCTTAGAAAGTGCGGCTTGAAAGAAC which incorporated, respectively, *Bam*HI and *Eco*RI cloning sites into the Ad7PB amplicon. The resulting construct, called pGST–Ad7PB, contained the Ad7PB open reading frame downstream of the *S. japonicum* GST gene. Expression from this vector is driven by the inducible Ptac promoter.

### Expression and purification of recombinant GST–Ad7PB

The expression vector pGST–Ad7PB containing the GST–Ad7PB expression cassette was used to transform *E. coli* BL21 (λDE3). Transformed bacteria were grown in 1 L shake-flask cultures in the presence of 100 $\mu g \cdot mL^{-1}$ ampicillin to a $D_{600} = 1.2–1.5$ and induced with 0.1 mM (final) isopropyl thio-β-D-galactoside. The GST–Ad7PB fusion protein was purified by affinity chromatography on glutathione agarose (glutathione–Sepharose 4B, Pharmacia), according to the method of Rhim *et al* [27]. Briefly, induced total cell pellets from 1 L of culture were resuspended in 4 mL EBC buffer (50 mM Tris/HCl pH 8.0, 120 mM NaCl, 0.5% NP-40) containing 5 mM dithiothreitol. Lysates were prepared by homogenization (Polytron homogenizer, Kinematica GmbH) in the presence of 2 $mg \cdot mL^{-1}$ lysozyme (Sigma). Lysates were clarified by centrifugation at 12 000 *g* (SS-34 rotor, Sorvall) and supernatants were loaded on a 200-μL glutathione-Sepharose 4B column prewashed with EBC buffer. The column was washed with EBC buffer containing 200 mM NaCl to strip protein bound nonspecifically to the column. The fusion protein was eluted with glutathione elution buffer (10 mM GSH in 50 mM Tris/HCl pH 8.0). Two-hundred-microliter fractions were collected and analyzed on a reducing polyacrylamide gel. Protein concentrations were determined by the Bio-Rad Protein Assay reagent, and peak fractions were stored at 4 °C for further analysis.

### Factor Xa-mediated cleavage of GST tag

The pGEX3X vector provides for a factor Xa cleavage site (Ile-Glu-Gly-Arg, with cleavage occurring after Arg) between GST and the fusion partner. Approximately 3 μg of affinity purified GST–Ad7PB were cleaved at room temperature for various time-points with 1 U of factor Xa (Sigma) in cleavage buffer consisting of 50 mM Tris/HCl (pH 7.5), 150 mM NaCl and 1 mM $CaCl_2$. The cleavage reaction was terminated by addition of Laemmli buffer and analyzed on a 10% SDS/PAGE gel.

For EM analysis, GST–Ad7PB fusion protein was subjected to complete cleavage (verified by SDS/PAGE analysis), followed by GST–agarose separation to remove uncleaved material. Briefly, 10 μg of GST–Ad7PB were digested with factor Xa as described above. Digested reaction products were loaded onto a 200-μL glutathione–Sepharose 4B column prequilibrated with EBC buffer. The eluate was collected. The column was then washed with EBC buffer to elute any remaining cleaved Ad7PB, leaving any residual uncleaved GST–Ad7PB or GST adhering to the column. The eluate and wash-off fractions were then pooled, and concentrated with a Centricon-30 (Amicon) to a volume of 100 μL. The concentrated sample was subjected to EM analysis and to N-terminal sequencing (see below).

### N-Terminal sequencing of Ad7PB

Factor Xa cleaved (GST-free) Ad7PB were blotted on to a PVDF membrane. N-Terminal peptide sequencing of the Ad7PB was performed by automated Edman degradation and HPLC using a Model 476A Protein Sequencer (Applied Biosystems).

### Electron microscopy of GST–Ad 7PB and Ad7PB

GST–Ad7PB and factor Xa-cleaved GST–Ad7PB were dialyzed against water. Protein at a concentration of about 0.1 $mg \cdot mL^{-1}$ was adsorbed to the clean face of carbon on mica (the carbon–mica interface) and then the carbon film with adsorbed protein

was floated onto a solution of 1% sodium silicotungstate. A grid was placed on top of the carbon film which was then picked up from the top with a small piece of newspaper and air-dried. The samples were photographed in a JEOL 1200 EXII electron microscope at 100 kV under low-dose conditions at a nominal magnification of 40 000×.

For image analysis, two negatives of each sample were selected and digitized using an Optronics microdensitometer with a pixel size of 25 μm. We selected 1000 particles of Ad7PB and 600 particles of GST–Ad7PB using XIMDISP [28]. The particles were cut out of the field in squares of 64 × 64 pixels and filtered between 250 and 15 Å. All particles were centered using a circular object with the same diameter as the PB. Using the multivariate statistical analysis and the classification method implemented in SPIDER [29], all particles were classified into different subgroups ('class averages'). The Ad7PB images were very homogenous and 80% segregated into pentameric subgroups, the other 20% being side views or tilted views. The GST–Ad7PB group of images was much more variable, and only 50% of the particles segregated into pentameric subgroups.

### Size analysis of GST–Ad7PB

To estimate the size of GST–Ad7PB, it was subjected to electrophoresis under nondenaturing and nonreducing conditions on a 8% separating gel with a 5% stacking gel. A number of high molecular mass proteins (Pharmacia) were included on the gel to provide size references. These were catalase (232 kDa), ferritin (440 kDa), thyroglobulin (660 kDa) and blue dextran (2 mDa).

### DNA retardation by GST–Ad7PB

A gel-shift assay was performed to test whether GST–Ad7PB bound a bifunctional linker peptide derived from the adenovirus fiber protein. This peptide, designated FK20 [MTKRVRLSDSFNPVYPYEDEK(1–20)], was obtained by solid-phase synthesis, purified by RP-HPLC and stored dry at −20 °C. It contains the first N-terminal 20 amino acids of Ad7 fiber followed by 20 lysines. It binds PB protein due to the NPVYPY(12–17) sequence from Ad fiber [1,30] and is able to attach and compact DNA through the C-terminal polylysine domain. In addition, it contains the nuclear localization signal of the fiber protein, KRVR [30,31].

Complexes between GST–Ad7PB and FK20 were prepared by incubating GST–Ad7PB with FK20 at room temperature for 30 min. At the end of this time period, 1 μg of DNA was added to allow to complex via the C-terminal polylysine chain. Binding of plasmid by the GST–Ad7PB–FK20 complex was examined by analysis of the electrophoretic mobility of the plasmid DNA, using a 1% Tris/acetate/EDTA/agarose gel.

### Ad7PB-mediated gene transfer

Adenovirus-susceptible human kidney epithelial cells (293 cells) were grown in DMEM containing 10% fetal bovine serum. Cells were maintained at 37 °C in the presence of 5% $CO_2$. GST–Ad7PB protein (5 and 10 μL corresponding to 1 and 2 μg of recombinant protein) was incubated with 1 μg of FK20 peptide for 30 min at room temperature. A reporter gene construct (pCMV-luc) containing the human cytomegalovirus immediate-early promoter cloned upstream of the firefly luciferase gene in plasmid pXP2 [32] was then added to the PB–FK20 linker complex, and the mixture was incubated for 30 min at room temperature (pCMV-luc was generated using standard recombinant DNA methods; not shown).

Cells were plated at a density of $2 \times 10^5$ per well in a 24 well plate, washed with serum-free medium and exposed to 100 μM chloroquine for 1 h. PB-DNA complexes were then added to cells in triplicate and incubated for 3 h at 37 °C in the presence of 5% $CO_2$. The PB–DNA complexes were removed at the end of 3 h, fresh complete medium was added, and the cells were incubated for an additional 60 h. At the end of this period, cells were washed with 1 × NaCl/$P_i$ and lysed in 100 μL reporter lysis buffer (Promega). Lysates were clarified by centrifugation at 5000 *g* and 20 μL of the clarified supernatants were assayed for luciferase activity using a microplate luminometer (LumiCount Model AL10000, Packard) in combination with the Luciferase Assay System (Promega). The results are expressed in relative light units (RLU) per microgram of cellular protein, as estimated using the Bio-Rad Protein Assay reagent.

## RESULTS

### *Ad7PB* gene sequence

Due to our interest in the use of the Ad3PB protein as a gene delivery system [15], we set out to examine whether the PB protein from a second, related strain of adenovirus might also have potential as a gene transfer vector. We therefore sequenced the gene coding for Ad7PB, because Ad7 is known to be closely related to Ad3, and also because Ad7 has previously been reported to have the ability to form dodecahedra, in a manner similar to Ad3 [26].

PCR amplification of the *Ad7PB* gene from Ad serotype 7 genomic DNA yielded a product of 1632 bp in length. The 544-amino-acid sequence of the *Ad7PB* gene was deduced from the nucleotide sequence and aligned with Ad2 and Ad3 PBs; Ad7 and Ad3 PB showed 99% identity at the amino-acid level (Genbank accession nos AAF37000and S41389, respectively), while Ad7 and Ad2 PB (Genbank accession P03276) were more divergent (77% predicted amino-acid identity). Both integrin-binding motifs, RGD (amino acids 329–331) and LDV (amino acids 296–298) were found to be conserved in Ad7PB. Also conserved was the RLSNLLG sequence (amino acids 263–269), identified as a putative fiber-binding domain on Ad2PB [1,33]. Sequences in Ad7PB flanking the RGD domain, a region known to exhibit considerable variation among Ad serotypes [34], were found to be almost identical to those found in Ad3PB (except for an asparagine residue at position 326 in Ad7PB vs. an aspartate at the corresponding location in Ad3 PB); in contrast, this region of Ad7PB is quite divergent from its counterpart in Ad2 (as previously noted by Karayan *et al* [34]).

### Expression of Ad7PB in *E. coli* and purification by affinity chromatography

In order to further study the Ad7PB protein, we decided to express the molecule as a GST fusion protein in *E. coli*. We selected this expression system because it offers several advantages, including ease-of-use and detection, single-step purification and removal of the fusion partner (GST) using appropriate protease cleavage (e.g., factor Xa). In addition, the GST leader is believed to assist the fusion partner in folding and in its expression in the soluble form.

GST–Ad7PB was expressed in *E. coli* in amounts up to 5 $mg \cdot L^{-1}$ of culture. The fusion protein was soluble and was

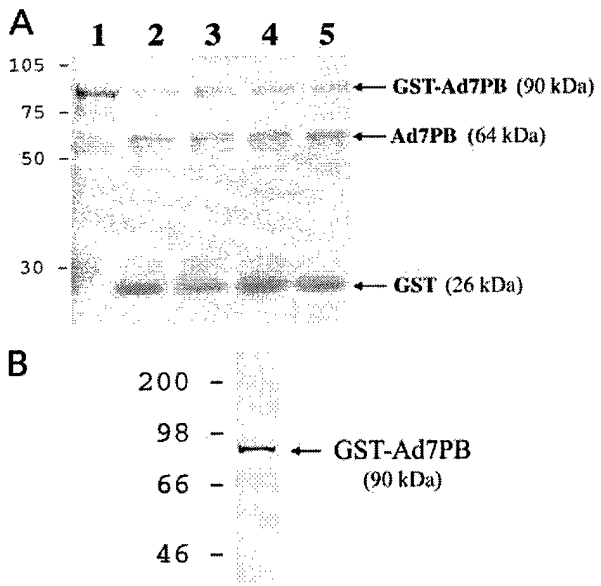


**Fig. 1. Purification of GST–Ad7PB.** (A) Factor Xa-mediated cleavage of GST–Ad7PB. GST–Ad7PB was incubated at room temperature with 1 U of factor Xa in 1 × cleavage buffer. Two-microgram equivalents of the protein were removed at various time-points and analyzed by electrophoresis on a 4–15% SDS-polyacrylamide gel (Bio-Rad). The gel was then stained with Coomassie brilliant blue. Uncleaved starting material (intact GST–Ad7PB, ≈90 kDa) is shown in lane 1, while cleaved Ad7PB (≈ 65 kDa) can be seen in the other lanes (lanes 2–5 represent 30, 45, 60 and 120 minute digestion with factor Xa). In all lanes, the presence of free GST protein (≈ 26 kDa) can observed; this is particularly pronounced after factor Xa cleavage. Numbers on the left represent molecular mass markers (figures in kDa). (B) Detection of GST–Ad7PB with an anti-Ad 3 PB Ig. Purified, full-length (not factor Xa-cleaved) recombinant GST–Ad7PB protein (2 μg) was electrophoresed on a 4–15% SDS-polyacrylamide gel (Bio-Rad), and an immunoblot was performed using a polyclonal rabbit antiserum directed against the adenovirus type 3 PB protein (this antiserum was generated in the Chroboczek lab., and used at a 1 : 100 000 dilution). Bound antibody was visualized using the ECL™ system (Amersham Pharmacia); numbers on the left represent molecular mass markers (figures in kDa).

purified from clarified bacterial lysates by single-step affinity chromatography on a glutathione–Sepharose 4B column. A 90-kDa band corresponding to the combined molecular masses of GST (26 kDa) and Ad7PB (64 kDa) was detected on a 4–15% SDS/PAGE (Fig. 1A, lane 1). This protein reacted with a polyclonal antiserum raised against the Ad3PB protein (Fig. 1B) and with an anti-GST Ig (data not shown), indicating that an authentic GST–Ad7PB protein was produced (note that Ad3PB is 99% identical to Ad7PB at the amino-acid level; thus a polyclonal antibody directed against Ad3PB can be expected to also recognize Ad7PB).

The GST–Ad7PB fusion protein could be cleaved with factor Xa to release the PB from the fusion protein. Factor Xa mediated cleavage of GST–Ad7PB at the Ile-Glu-Gly-Arg recognition site between GST and the beginning of Ad7PB yielded a protein of 64 kDa, corresponding to the expected molecular mass of the Ad7PB (Fig. 1A, lanes 2–5). N-Terminal peptide sequencing of the purified, factor Xa-cleaved Ad7PB protein confirmed that the purified protein did indeed correspond to Ad7PB (data not shown), and it also revealed the presence of copurified 60-kDa GroEL chaperone protein within the protein preparation (this is presumably present at low levels; Fig. 1A). However, total cleavage of the fusion protein could not be obtained within the 2-h reaction (see Fig. 1A). Thus, more complete digestion was required for studies in which GST-free Ad7PB was used (i.e. electron microscopy experiments; see below).

## Structural characterization of Ad7PB proteins

Analysis of GST–Ad7PB by nondenaturing SDS/PAGE revealed that the recombinant protein migrated considerably more slowly than would have been expected for a GST–Ad7PB protein monomer (data not shown). This suggested that the recombinant GST–Ad7PB protein might have become organized into a pentameric configuration. Glutaraldehyde cross-linking and analysis by denaturing SDS/PAGE confirmed this possibility (data not shown), and we therefore undertook an EM analysis of both the recombinant GST–Ad7PB protein and also of the cleaved, GST-free Ad7PB protein.

Ad7PB and GST–Ad7PB were prepared for electron microscopy by negative staining. For EM analysis, GST–Ad7PB fusion was subjected to complete cleavage (verified by SDS/PAGE analysis), followed by GST–Sepharose separation to remove uncleaved material (see Materials and methods). Figure 2 shows pictures of fields of the two samples as well as selected untreated and averaged images in a gallery. The Ad7PB sample (Fig. 2A) contained homogeneous particles that could easily be classified in class averages that showed fivefold symmetry (e.g. Fig. 2A, bottom right) clearly showing the five subunits in the PB. This pentamer has a width of 100 Å the same as the width of the Ad3 PB [15]. The GST–Ad7PB sample was much less homogeneous because, although the PB part of the molecule was always the same and identical to the PB part in Ad7PB alone, the GST subunits seem to be rather flexibly linked to the PB, leading to a rather high number of class averages. Figure 2B shows a field of the sample and a gallery, together with a selected untreated image at the top and the class average it belongs to at the bottom. Because of the flexible PB–GST linkage, the class averages only clearly show two attached GST molecules at one time. The other three GST molecules are either not well embedded in the stain or not always located at exactly the same position compared to the other GST subunits, leading to loss of the signal in the average. From the class averages it can also be seen that the actual diameter of the GST–Ad7PB molecule is much higher than that of the PB alone and also much higher than the diameter of a globular complex with a corresponding mass. Neither the cleaved nor the uncleaved GST–Ad7PB formed dodecamers, as did the baculovirus produced Ad3PB [15]. However, the formation of pentamers by both Ad7PB and GST–Ad7PB indicates that pentamer formation by the *E. coli*-derived recombinant proteins is dependent upon the interaction of the PBs (i.e. pentamer formation is not dependent upon the presence of GST).

## DNA retardation by GST–Ad7PB

GST–Ad7PB was effective in retarding the electrophoretic mobility of plasmid DNA, in the presence of the FK20 linker peptide, in a dose-dependent manner (Fig. 3). In the absence of the FK20 linker peptide, GST–Ad7PB alone failed to retard plasmid DNA (lanes 2–4). The migration pattern of pCMV-luc in these lanes was similar to the untreated plasmid in lane 1, which shows the mobility of free, supercoiled plasmid DNA. The binding and consequent retardation of pCMV-luc by the

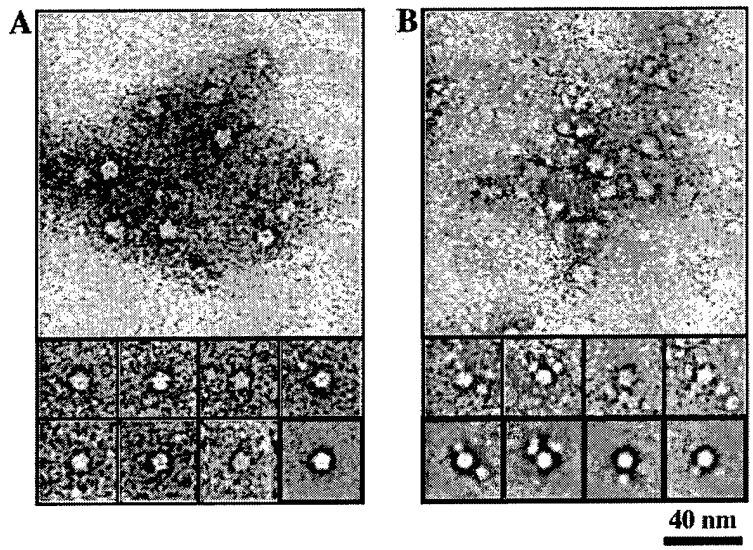


**Fig. 2. Electron micrographs of negatively stained GST–Ad7PB and factor Xa cleaved Ad7PB.** (A) Shows a field of factor Xa cleaved Ad7PB at the top and seven selected images of individual molecules. At the bottom right is a class average of 15 averaged raw images (see Materials and methods). (B) Shows a field of untreated GST–Ad7PB and four class averages calculated by summing 15 raw images. For each class average in the lower panel one of the raw images used to calculate the average is shown in the upper panel. The bar represents 40 nm (equals 400 Å).

GST–Ad7PB–FK20 complex is evident in lanes 5, 6 and 7 which contain increasing amounts (1, 2 and 4 μg, respectively) of GST–Ad7PB with a fixed amount of FK20 peptide. Plasmid DNA binding was dependent on Ad7PB and not on the GST moiety, as the mobility of plasmid DNA was unaltered in the presence of FK20 peptide plus GST alone (lanes 8, 9 and 10 which contain 1, 2 and 4 μg of GST, respectively).

## GST–Ad7PB-mediated transfection

The ability of the GST–Ad7PB fusion protein to mediate gene transfer into cultured human cells was assessed by adding a complex of GST–Ad7PB plus FK20 preincubated with the luciferase reporter plasmid DNA (GST–Ad7PB–FK20–DNA) to 293 cells. Expression of luciferase was observed in 293 cells transfected with the GST–Ad7PB–FK20–DNA complex, either in the presence or absence of chloroquine (Fig. 4, lanes 4 and 5). Gene transfer by the GST–Ad7PB–FK20–DNA complex was somewhat less efficient in the presence of chloroquine (lane 5) than in its absence (lane 4). This may be due, in part, to

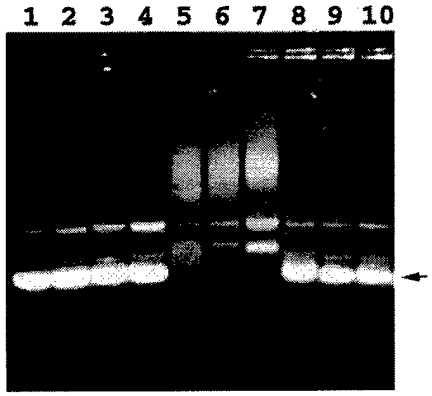


**Fig. 3. GST–Ad7PB-mediated DNA retardation via FK20 linker.** GST–Ad7PB or GST alone, was incubated with a luciferase reporter plasmid (pCMV-luc), in the presence and absence of 0.5 μg of the FK20 linker peptide. DNA–protein complexes were analysed by electrophoresis on a 1% agarose gel in 1 × Tris/acetate/EDTA. DNA was visualized using ethidium bromide and a photograph of the resulting gel is shown. Lane 1: untreated DNA incubated in buffer (this shows the mobility of free, supercoiled plasmid DNA; see arrow). Lanes 2, 3 and 4 contain plasmid DNA that was preincubated with 1, 2 and 4 μg of GST–Ad7PB (no FK20), while lanes 5, 6 and 7 contain DNA plus FK20 plus increasing amounts of GST–Ad7PB (1, 2 or 4 μg, respectively). Finally, lanes 8, 9 and 10 contain plasmid DNA plus GST (1, 2 or 4 μg, respectively) plus FK20.

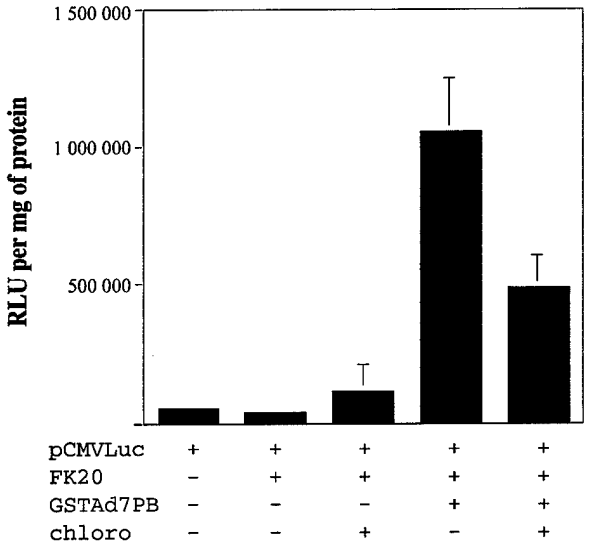


**Fig. 4. GST–Ad7PB-mediated transfection of 293 cells.** 293 cells were incubated with pCMV-luc and luciferase expression was measured in cell lysates collected 60 h after transfection. Lane 1, pCMV-luc added in the absence of GST–Ad7PB (control). Lanes 2 and 3, pCMV-luc and FK20 linker peptide added, in the absence (lane 2) or presence (lane 3) of chloroquine. Lanes 4 and 5, pCMV-luc plus FK20 plus GST–Ad7PB protein added, in the absence (lane 4) or presence (lane 5) of chloroquine. Luciferase activity is expressed in terms of relative light units (RLU) per mg of total protein in the cell lysates. Bars represent the standard error of mean values. The experiment was performed in triplicate and the results shown are representative of three experiments which yielded similar data.

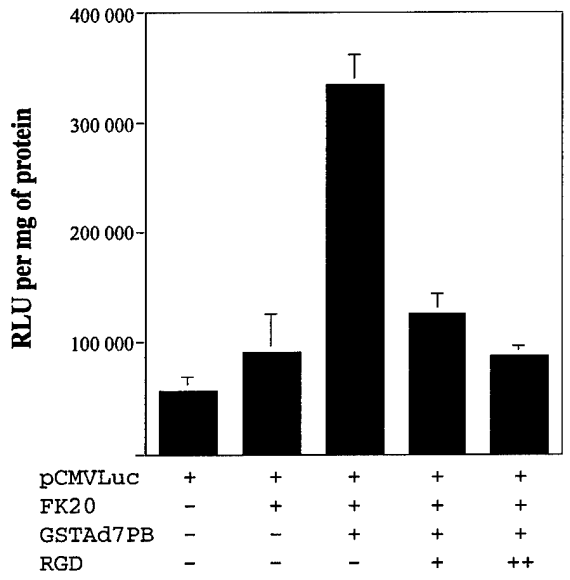


**Fig. 5. Inhibition of GST–Ad7PB-mediated transfection of 293 cells by an RGD-containing peptide.** 293 cells were incubated with pCMV-luc and luciferase expression was measured in cell lysates collected 60 h later. Lane 1, cells treated with pCMV-luc in the absence of GST–Ad7PB (control). Lane 2, Cells exposed to a complex of pCMV-luc and FK20 linker only. Lanes 3–5, Cells exposed to a complex of pCMV-luc and FK20 linker plus GST–Ad7PB protein, in the absence (lane 3) or presence (lanes 4 and 5) of an RGD-containing peptide (NITRGDTYI; added at 10 or 100 μg to lanes 4 and 5, respectively). Luciferase activity is expressed in terms of relative light units (RLU) per mg of total protein in the cell lysates. Bars represent the standard error of mean values. The experiment was performed in triplicate and the results shown are representative of three experiments which yielded similar data.

possible toxic effects of chloroquine under the conditions used. In any event, a much lower level of luciferase activity was detectable in cells transfected with complexes containing FK20 peptide plus DNA (i.e. complexes lacking the GST–Ad7PB protein). This is consistent with our previous finding that an analogous peptide derived from the adenovirus type 2 fiber protein can mediate DNA transfer into some human cell types [35].

While Ad7-derived FK20 peptide could mediate a low level of DNA uptake into 293 cells, perhaps due to the presence of a tyrosine-based motif (NPXY) that may function as an internalization signal involved in receptor-mediated endocytosis [36–38], DNA delivery was much more efficient when the GST–Ad7PB protein was added to the transfection complex, and transfection also occurred in the absence of chloroquine (Fig. 4).

To investigate the specificity of DNA transfection by the GST–Ad7PB–FK20–DNA complex, cells were preincubated in the presence of an excess of an RGD-containing peptide derived from the Ad7PB (NITRGDTYI) prior to the addition of the GST–Ad7PB–FK20–DNA complex. This resulted in a strong dose-dependent inhibition of luciferase expression in the transfected cells (Fig. 5, lanes 3–5), suggesting that the GST–Ad7PB protein facilitates DNA uptake via an integrin-dependent pathway.

## DISCUSSION

The adenovirus PB may be an ideal molecule to exploit as a gene transport vehicle, because it is able to interact in a selective manner with cell-surface integrins to effect internalization. We sequenced the full-length gene coding for Ad7PB protein and found it to be 99% identical to the Ad3PB at the amino-acid level. Ad7PB was also found to retain the integrin-binding peptide motifs present in PB proteins from several other adenovirus serotypes (RGD and LDV), as well as residues involved in penton-fiber binding and pentamerization factors that were critical for DNA delivery.

Expression of Ad7PB as a C-terminal fusion with *S. japonicum* GST in *E. coli* BL21 cells yielded soluble protein that could be purified from bacterial lysates by a single-step affinity chromatography. To our knowledge, this is the first report of the production of stable adenoviral pentons from *E. coli*. Bai *et al* [6,14]. have reported bacterial expression of Ad2PB and Ad12PB. In both cases, the PB was found to localize in *E. coli* as insoluble inclusion bodies. Our method represents an improvement over the method reported by Bai and coworkers, both in the soluble nature of expression and also in terms of ease of down-stream processing.

Structural characterization of Ad7PB by negative stain electron microscopy revealed that the *E. coli*-derived protein was pentameric, like the native form of this protein. Although the PBs formed from cleaved, GST-free, Ad7PB were more symmetrical, the GST-tagged protein retained the inherent spontaneous capability of forming pentamers. The fact that a 26-kDa addition (GST) at the N-terminus of PB did not inhibit pentamer formation indicates that signals for pentamerization may be located distal to the PB N-terminus. Indeed, most of the residues implicated so far in pentamerization are present at the C-terminus of PB (Y553 and K556) or are located far from the N-terminus (W119) [33]. In addition, the ability of GST–Ad7PB to bind a fiber-like peptide (FK20), as reflected by the results of our DNA retardation experiments (Fig. 3), suggests that the presence of the GST moiety does not interfere with fiber-binding of Ad7PB. Thus, the conformation of the GST–Ad7PB fusion protein appears to be biochemically indistinguishable from that of its native (unfused) counterpart.

N-Terminal sequencing of GST–Ad7PB also revealed an association of the 60-kDa chaperonin GroEL with GST–Ad7PB. *E. coli* GroEL is known to bind a number of proteins expressed as GST fusions in bacteria [5,39] and to aid the formation of native structures. Battistoni *et al* [39]. have demonstrated that *E. coli* chaperonins are able to interact with nascent GST. It is possible that GroEL plays an analogous role in the folding of GST–Ad7PB and assists in the formation of pentamers.

Gene transfer efficiency by the GST–Ad7PB–FK20–DNA complex was found to exhibit significant variation in different experiments. For example, the efficiency of gene expression in Fig. 4, lane 4 is roughly threefold greater than that in Fig. 5, lane 3, even though the cells in these experiments were exposed to the same reagent (GST–Ad7PB + FK20 + pCMV-luc), in the absence of chloroquine. We attribute this variation to the fact that the large macromolecular complex represented by GST–Ad7PB–FK20–DNA is held together by at least two separate interactions: a protein–peptide interaction between GST–Ad7PB and FK20, and an electrostatic interaction between FK20 and DNA. The latter interaction is likely to be particularly susceptible to slight differences in storage conditions and ionic strength of any buffers used. Slight fluctuations in pH may also alter the strength of the various interactions which hold the GST–Ad7PB–FK20–DNA complex together.

Nonetheless, GST–Ad7PB was found to transfect 293 cells in an integrin-dependent fashion (as expected). Furthermore, GST–Ad7PB-mediated gene transfer was not improved by the

presence of chloroquine (indeed, it was enhanced in the absence of the drug; Fig. 4, lanes 4 and 5). This suggests that GST–Ad7PB-mediated gene transfer occurs either by a lysosome-independent pathway, as described for fibroblast growth factor and HIV-1 Vpr [40,41], or as a consequence of PB-mediated endosome escape in 293 cells [42].

In previous experiments using recombinant Ad3PB dodecahedra prepared from insect cell lysates, we obtained levels of reporter gene expression in transfected 293 cells that were approximately 1000-fold higher than the levels reported here, using the *E. coli*-derived GST–Ad7PB fusion protein [15]. Similarly, the level of transfection obtained with commercial transfection reagents such as lipofectamine or DOTAP was 10–20 times higher than the level reported here.

The difference in transfection efficiency between the Ad3PB dodecahedra and the recombinant GST–Ad7PB protein preparations used here cannot be attributed simply to the presence of the GST moiety, as factor Xa-cleaved GST-free Ad7PB protein mediated a similar level of DNA transfer to that obtained with the GST–Ad7PB fusion (data not shown). Thus, the differences between our current findings and those reported with the insect cell-derived Ad3 base dodecahedra preparations may be due to inherent differences in structural features of the pentameric PB vs. dodecahedra. GST–Ad7PB assumes a pentameric configuration that possesses a total of five RGD motifs (integrin-binding domains) and five binding sites for the FK20 linker peptide. This may explain why base dodecahedra (60 RGD motifs and 60 binding sites for the FK20 peptide) are more efficient gene delivery systems than PB [15]. We are currently devising strategies to modify *E. coli*-expressed PB in such a manner as to facilitate the formation of dodecahedra.

Overall, the results reported here establish the potential utility of *E. coli*-derived Ad7PB as a gene delivery agent. Further experiments, including mutagenesis of the residues flanking the RGD motif, will be required in order to optimize this technology, and to exploit its potential for integrin-mediated gene delivery to specific target cell populations [43].

## ACKNOWLEDGEMENTS

The authors thank Drs Jack Maniloff and George Kampo for assistance with DNA sequence analysis, Karen Jensen for assistance with electron microscopy, and Brian van Wuyckhuyse for assistance with protein sequencing. Sequences described in this paper have been deposited with GenBank (accession nos AD001675and AAF37000). The study was funded by NIH grant No. R21AI44362, and by award no. DAMD17-99-1-9361 from the Department of the Army (to S. D.) and by an award from the French Cancer Society/ARC (to J. C.). The US Army Medical Research Acquistion Activity, 820 Chandler Street, Fort Detrick MD 21702-5104 is the awarding and administering acquisition office, and the information content of this article does not necessarily reflect the position or the policy of the US Government; no official endorsement should be inferred.

## REFERENCES

1. Caillet-Boudin, M.L. (1989) Complementary peptide sequences in partner proteins of the adenovirus capsid. *J. Mol. Biol.* **208**, 195–198.
2. Devaux, C., Caillet-Boudin, M.L., Jacrot, B. & Boulanger, P. (1987) Crystallization, enzymatic cleavage, and the polarity of the adenovirus type 2 fiber. *Virology* **161**, 121–128.
3. Bergelson, J.M., Cunningham, J.A., Droguett, G., Kurt-Jones, E.A., Krithivas, A., Hong, J.S., Horwitz, M.S., Crowell, R.L. & Finberg, R.W. (1997) Isolation of a common receptor for Coxsackie B viruses and adenoviruses 2 and 5. *Science* **275**, 1320–1323.
4. Bergelson, J.M., Krithivas, A., Celi, L., Droguett, G., Horwitz, M.S., Wickham, T., Crowell, R.L. & Finberg, R.W. (1998) The murine CAR homolog is a receptor for coxsackie B viruses and adenoviruses. *J. Virol.* **72**, 415–419.
5. Thain, A., Gaston, K., Jenkins, O. & Clarke, A.R. (1996) A method for the separation of GST fusion proteins from co-purifying GroEL. *Trends Genet.* **12**, 209–210.
6. Bai, M., Harfe, B. & Freimuth, P. (1993) Mutations that alter an Arg-Gly-Asp (RGD) sequence in the adenovirus type 2 penton base protein abolish its cell-rounding activity and delay virus reproduction in flat cells. *J. Virol.* **67**, 5198–5205.
7. Goldman, M.J. & Wilson, J.M. (1995) Expression of alpha v beta 5 integrin is necessary for efficient adenovirus-mediated gene transfer in the human airway. *J. Virol.* **69**, 5951–5958.
8. Wickham, T.J., Mathias, P., Cheresh, D.A. & Nemerow, G.R. (1993) Integrins alpha v beta 3 and alpha v beta 5 promote adenovirus internalization but not virus attachment. *Cell* **73**, 309–319.
9. Wickham, T.J., Filardo, E.J., Cheresh, D.A. & Nemerow, G.R. (1994) Integrin alpha v beta 5 selectively promotes adenovirus mediated cell membrane permeabilization. *J. Cell Biol.* **127**, 257–264.
10. Chardonnet, Y. & Dales, S. (1970) Early events in the interaction of adenoviruses with HeLa cells. I. Penetration of type 5 and intracellular release of the DNA genome. *Virology* **40**, 462–477.
11. FitzGerald, D.J., Padmanabhan, R., Pastan, I. & Willingham, M.C. (1983) Adenovirus-induced release of epidermal growth factor and pseudomonas toxin into the cytosol of KB cells during receptor-mediated endocytosis. *Cell* **32**, 607–617.
12. Freimuth, P. (1996) A human cell line selected for resistance to adenovirus infection has reduced levels of the virus receptor. *J. Virol.* **70**, 4081–4085.
13. Hashimoto, Y., Kohri, K., Akita, H., Mitani, K., Ikeda, K. & Nakanishi, M. (1997) Efficient transfer of genes into senescent cells by adenovirus vectors via highly expressed alpha v beta 5 integrin. *Biochem. Biophys. Res. Commun* **240**, 88–92.
14. Bai, M., Campisi, L. & Freimuth, P. (1994) Vitronectin receptor antibodies inhibit infection of HeLa and A549 cells by adenovirus type 12 but not by adenovirus type 2. *J. Virol.* **68**, 5925–5932.
15. Fender, P., Ruigrok, R.W., Gout, E., Buffet, S. & Chroboczek, J. (1997) Adenovirus dodecahedron, a new vector for human gene transfer. *Nat. Biotech.* **15**, 52–56.
16. Yang, Y., Li, Q., Ertl, H.C. & Wilson, J.M. (1995) Cellular and humoral immune responses to viral antigens create barriers to lung-directed gene therapy with recombinant adenoviruses. *J. Virol.* **69**, 2004–2015.
17. Engelhardt, J.F., Simon, R.H., Yang, Y., Zepeda, M., Weber-Pendleton, S., Doranz, B., Grossman, M. & Wilson, J.M. (1993) Adenovirus-mediated transfer of the CFTR gene to lung of nonhuman primates: biological efficacy study. *Hum. Gene Ther.* **4**, 759–769.
18. Marshall, E. (1999) Gene therapy death prompts review of adenovirus vector. *Science* **286**, 2244–2245.
19. Aplin, A.E., Howe, A., Alahari, S.K. & Juliano, R.L. (1998) Signal transduction and signal modulation by cell adhesion receptors: the role of integrins, cadherins, immunoglobulin-cell adhesion molecules, and selectins. *Pharmacol. Rev.* **50**, 197–263.
20. Brooks, P.C., Clark, R.A. & Cheresh, D.A. (1994) Requirement of vascular integrin alpha v beta 3 for angiogenesis. *Science* **264**, 569–571.
21. Enenstein, J., Waleh, N.S. & Kramer, R.H. (1992) Basic FGF and TGF-beta differentially modulate integrin expression of human microvascular endothelial cells. *Exp. Cell Res.* **203**, 499–503.
22. Brooks, P.C., Montgomery, A.M., Rosenfeld, M., Reisfeld, R.A., Hu, T., Klier, G. & Cheresh, D.A. (1994) Integrin alpha v beta 3 antagonists promote tumor regression by inducing apoptosis of angiogenic blood vessels. *Cell* **79**, 1157–1164.
23. Humphries, M.J. (1990) The molecular basis and specificity of integrin-ligand interactions. *J. Cell Sci.* **97**, 585–592.
24. Newham, P. & Humphries, M.J. (1996) Integrin adhesion receptors: structure, function and implications for biomedicine. *Mol. Med. Today* **2**, 304–313.
25. Mathias, P., Wickham, T., Moore, M. & Nemerow, G. (1994) Multiple adenovirus serotypes use alpha v integrins for infection. *J. Virol.* **68**, 6811–6814.

26. Norrby, E. (1969) The structural and functional diversity of Adenovirus capsid components. *J. Gen. Virol.* **5**, 221–236.
27. Rhim, H., Echetebu, C.O., Herrmann, C.H. & Rice, A.P. (1994) Wild-type and mutant HIV-1 and HIV-2 Tat proteins expressed in *Escherichia coli* as fusions with glutathione S-transferase. *J. Acquir. Immune Defic. Syndr.* **7**, 1116–1121.
28. Crowther, R.A., Henderson, R. & Smith, J.M. (1996) MRC image processing programs. *J. Struct. Biol.* **116**, 9–16.
29. Frank, J., Radermacher, M., Penczek, P., Zhu, J., Li, Y., Ladjadj, M. & Leith, A. (1996) SPIDER and WEB: processing and visualization of images in 3D electron microscopy and related fields. *J. Struct. Biol.* **116**, 190–199.
30. Hong, J.S. & Engler, J.A. (1996) Domains required for assembly of adenovirus type 2 fiber trimers. *J. Virol.* **70**, 7071–7078.
31. Chelsky, D., Ralph, R. & Jonak, G. (1989) Sequence requirements for synthetic peptide-mediated translocation to the nucleus. *Mol. Cell. Biol.* **9**, 2487–2492.
32. Nordeen, S.K. (1988) Luciferase reporter gene vectors for analysis of promoters and enhancers. *Biotechniques* **6**, 454–458.
33. Hong, S.S. & Boulanger, P. (1995) Protein ligands of the human adenovirus type 2 outer capsid identified by biopanning of a phage-displayed peptide library on separate domains of wild-type and mutant penton capsomers. *EMBO J.* **14**, 4714–4727.
34. Karayan, L., Hong, S.S., Gay, B., Tournier, J.D., 'AngeacD, A.D. & Boulanger, P. (1997) Structural and functional determinants in adenovirus type 2 penton base recombinant protein. *J. Virol.* **71**, 8678–8689.
35. Zhang, F., Andreassen, P., Fender, P., Geissler, E., Hernandez, J.-F. & Chroboczek, J. (1999) A transfecting peptide derived from adenovirus fiber protein. *Gene Ther.* **6**, 171–181.
36. Chen, W.J., Goldstein, J.L. & Brown, M.S. (1990) NPXY, a sequence often found in cytoplasmic tails, is required for coated pit-mediated internalization of the low density lipoprotein receptor. *J. Biol. Chem.* **265**, 3116–3123.
37. Hsu, D., Knudson, P.E., Zapf, A., Rolband, G.C. & Olefsky, J.M. (1994) NPXY motif in the insulin-like growth factor-I receptor is required for efficient ligand-mediated receptor internalization and biological signaling. *Endocrinology* **134**, 744–750.
38. Paccaud, J.P., Reith, W., Johansson, B., Magnusson, K.E., Mach, B. & Carpentier, J.L. (1993) Clathrin-coated pit-mediated receptor internalization. Role of internalization signals and receptor mobility. *J. Biol. Chem.* **268**, 23191–23196.
39. Battistoni, A., Mazzetti, A.P., Petruzzelli, R., Muramatsu, M., Federici, G., Ricci, G. & Lo Bello, M. (1995) Cytoplasmic and periplasmic production of human placental glutathione transferase in *Escherichia coli*. *Protein Expr. Purif* **6**, 579–587.
40. Hu, G., Kim, H., Xu, C. & Riordan, J.F. (2000) Fibroblast growth factors are translocated to the nucleus of human endothelial cells in a microtubule- and lysosome-independent pathway. *Biochem. Biophys. Res. Commun* **273**, 551–556.
41. Kichler, A., Pages, J.C., Leborgne, C., Druillennec, S., Lenoir, C., Coulaud, D., Delain, E., Le Cam, E., Roques, B.P. & Danos, O. (2000) Efficient DNA transfection mediated by the C-terminal domain of human immunodeficiency virus type 1 viral protein R. *J. Virol.* **74**, 5424–5431.
42. Midoux, P., Mendes, C., Legrand, A., Raimond, J., Mayer, R., Monsigny, M. & Roche, A.C. (1993) Specific gene transfer mediated by lactosylated poly-L-lysine into hepatoma cells. *Nucleic Acids Res.* **21**, 871–878.
43. Mette, S.A., Pilewski, J., Buck, C.A. & Albelda, S.M. (1993) Distribution of integrin cell adhesion receptors on normal bronchial epithelial cells and lung cancer cells *in vitro* and *in vivo*. *Am. J. Respir Cell Mol Biol.* **8**, 562–572.

doi:10.1016/S0022-2836(03)00082-2 J. Mol. Biol. (2003) 326, 1475–1488

JMB Available online at www.sciencedirect.com SCIENCE DIRECT®

# Engineered Fibronectin Type III Domain with a RGDWXE Sequence Binds with Enhanced Affinity and Specificity to Human αvβ3 Integrin

**Julie Richards[1], Michelle Miller[1], Johanna Abend[1], Akiko Koide[2] Shohei Koide[2] and Stephen Dewhurst[1]***

[1]*Department of Microbiology and Immunology, University of Rochester Medical Center, 575 Elmwood Avenue, Box 672 Rochester, NY 14642, USA*

[2]*Department of Biochemistry and Biophysics, University of Rochester, 601 Elmwood Avenue, Box 672, Rochester NY 14642, USA*

**Corresponding author*

Fibronectin is an extracellular matrix protein with broad binding specificity to cell surface receptors, integrins. The tenth fibronectin type III domain (FNfn10) is a small, autonomous domain of fibronectin containing the RGE sequence that is directly involved in integrin binding. However, in isolation FNfn10 only weakly bind to integrins. We reasoned that high-affinity and high-specificity variants of FNfn10 to a particular integrin could be engineered by optimizing residues surrounding the integrin-binding RGD sequence in the flexible FG loop. Affinity maturation of FNfn10 to αvβ3 integrin, an integrin up-regulated in angiogenic endothelial cells and in some metastatic tumor cells, yielded αvβ3-binding FNfn10 mutants with a novel RGDWXE consensus sequence. We characterized one of the RGDWXE-modified clones, FNfn10-3JCLI4, as purified protein. FNfn10-3JCLI4 binds with high affinity and specificity to purified αvβ3 integrin. Alanine scanning mutagenesis suggested that both the tryptophan and glutamic acid residues following the RGD sequence are required for maximal affinity and specificity for αvβ3. FNfn10-3JCLI4 specifically stained αvβ3-positive cells as detected with flow cytometry and it inhibited αvβ3-dependent cell adhesion. As with the anti-αvβ3 antibody LM609, FNfn10-3JCLI4 can interfere with *in vitro* capillary formation. Taken together, these data show that FNfn10-3JCL14 is a specific, high-affinity αvβ3-binding protein that can inhibit αvβ3-dependent cellular processes similar to an anti-αvβ3 monoclonal antibody. These properties, combined with the small, monomeric, cysteine-free and highly stable structure of FNfn10-3JCLI4, may make this protein useful in future applications involving detection and targeting of αvβ3-positive cells.



*Keywords:* phage display; scaffold; fibronectin type III domain; integrin; RGD

## Introduction

Phage display technology, in which combinatorial peptide libraries are expressed on the surface of bacteriophage, has been used to select for peptide ligands for a wide variety of substrates. An important variant of traditional phage display is the expression of polypeptide scaffolds on the surface of the phage that display random peptides in structurally defined exposed loops. Most of these scaffolds are composed mainly of beta sheets, although randomization of the exposed surfaces of alpha-helices (zinc fingers, staphylococcal protein A) have also been reported. Scaffolds self-fold into appropriate three-dimensional conformations on the phage surface. Unlike peptides displayed on pIII or pVIII, affinity and conformation of the modified scaffolds generally are maintained when expressed in the absence of the phage particle.[1] Scaffolds improve on traditional peptide phage display because the scaffold protein can be

Present address: A. Koide & S. Koide, Department of Biochemistry and Molecular Biology, University of Chicago, 920 E. 58th Street, Chicago, IL 60637, USA.

Abbreviation used: pfu, plaque-forming units.

E-mail address of the corresponding author: stephen_dewhurst@urmc.rochester.edu

expressed independently for stable, high-affinity binding to the target ligand, whereas peptide ligands typically tend to bind with lower affinities. It should be noted, however, that the measured binding affinities of peptide ligands for their target proteins can vary considerably, with some peptides having measured affinities in the low nanomolar range, and many others having affinities in the medium to high micromolar range.[2–4] Scaffold proteins selected for binding to a variety of target proteins have been previously identified with affinities ($K_d$) that also vary across a similar concentration range. In contrast, monoclonal antibodies generally bind with affinities in the picomolar to low nanomolar range and exhibit demonstrably strong preference for their target over other related molecules. The tenth fibronectin type III domain (FNfn10) contains the RGD integrin-binding sequence in the highly flexible loop connecting the F and G β-strands (FG loop).[5,6] FNfn10 was developed as a scaffold for phage display of peptides because of its small size (94 residues), monomeric assembly, and ability to retain its global fold while exposed loops were randomized.[7] In addition, FNfn10 lacks cysteine residues and requires no post-translational modification, allowing for large-scale bacterial expression. We reasoned that since fibronectin binds αvβ3 integrin *in vivo* through its RGD sequence, modification of amino acid residues surrounding the RGD sequence in the FG loop might result in a modified FNfn10 with higher affinity and/or specificity for αvβ3.

αvβ3 (CD51/CD61) is a member of the integrin family of cell surface adhesion receptors. Over 20 different αβ integrin heterodimers exist, each with different tissue and ligand specificities. Normal tissue distribution of αvβ3 is generally limited to high levels of expression on osteoclasts, but is also observed on platelets, megakaryocytes, kidney, vascular smooth muscle, placenta, dendritic cells,[8] and in varying amounts on normal endothelium.[9] Divalent cations are required for integrin ligand binding; in many cases, calcium alone is not sufficient to promote adhesion. αvβ3 integrin is a multifunctional cell surface receptor that has pleiotropic roles in normal cell growth and survival, and which can contribute to oncogenesis. Consistent with this, upregulation of αvβ3 expression has been observed on the endothelial cells of angiogenic vessels, and binding of αvβ3 to the basement membrane is a critical step in the angiogenesis induced by basic fibroblast growth factor and tumor necrosis factor alpha.[10] Expression of αvβ3 has also been implicated in tumor invasion, and it has been shown that αvβ3 binds matrix metalloproteinase-2 (MMP-2) and presents MMP-2 on the surface of invasive carcinomas and on invasive angiogenic endothelial cells.[11,12] αvβ3 also regulates cell growth and survival, since ligation of this receptor can, under some circumstances, induce apoptosis in tumor cells.[13] Furthermore, disruption of cell adhesion with anti-αvβ3 antibodies, RGD peptides, and other integrin antagonists has been shown to slow tumor growth.[14–16] Finally, the selective upregulation of αvβ3 expression on tumor blood vessels is also being explored as the basis for imaging of neoplastic lesions, and the αvβ3-specific antibody LM609 has been successfully used for this purpose *in vivo*.[17] Molecules capable of binding with high specificity to αvβ3 integrin have potential utility in several applications; as a consequence, αvβ3 has been a frequent target for drug discovery and selection of new binding ligands.

In contrast to α5β1, which binds to only fibronectin, αvβ3 binds to a wide range of RGD-containing integrin ligands, including but not limited to fibronectin, vitronectin, osteopontin, von Willebrandt factor, and fibrinogen.[9] Perhaps because αvβ3 binds a variety of RGD sequences, previous attempts to use phage display to elucidate broader RGD consensus sequences have been unsuccessful. At least one phage display scaffold, CTLA-4, was used to screen for αvβ3-binding polypeptides. This resulted in the identification of phage clones that could be used to stain human umbilical vein endothelial cells in a flow cytometric assay. However, no consensus binding sequence beyond RGD was reported and the affinity and specificity of the purified protein was not assessed.[18] Here, we demonstrate that derivatives of FNfn10 with high affinity and specificity for αvβ3 can be selected from a partially randomized FNfn10 library, expressed on the surface of phage M13. All αvβ3-binding FNfn10 clones were found to contain a RGDWXE consensus sequence, and the purified monomeric FNfn10-derived proteins were found to have similar characteristics to αvβ3-specific monoclonal antibodies, with respect to their stability, specificity, affinity, and effects on cell adhesion and *in vitro* capillary tube formation.

## Results

### Screening of the JCFN-RGD phage display library for αvβ3 binding resulted in selection of phage clones containing RGDWXE in the FG loop of displayed FNfn10

In the FNfn10 structure, the FG loop corresponds to residues 78–87, and the RGD sequence to residues 79–81 (residue numbering according to the Protein Data Bank entry 1TTG).[5] The five residues immediately adjacent to the RGD sequence in the FG loop were modified (Figure 1(a)). The JCFN-RGD (XRGDXXXX) library contained approximately $1.5 \times 10^9$ independent clones, sufficiently large to include all possible sequences. The library was amplified in 0.0 mM, 0.1 mM, or 1.0 mM IPTG to vary FNfn10 copy number and screened for binding to αvβ3 integrin. After three rounds of biopanning, 100–1000-fold increased recovery of phage was observed compared to the initial library (data not shown). Of 20 phage clones sequenced,

(a)

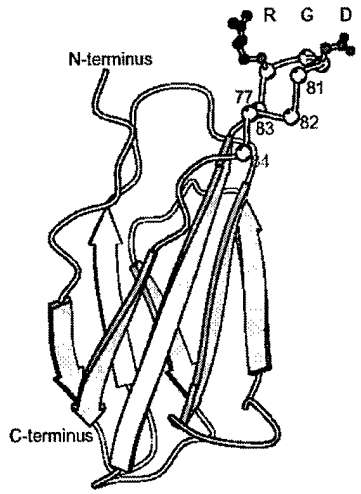


(b)

| | | | |
|---|---|---|---|
| **2JCAV1** | LRGDWSED | **3JCNI1** | PRGDWIEF |
| **2JCAV2** | VRGDWYEY | 3JCNI2 | GRGDSPAS |
| 2JCAV3 | VRGDCSSS | 3JCNI3 | GRGDDDRL |
| 2JCAV4 | GRGDLCDF | 3JCNI4 | GRGDYVLG |
| 2JCAV5 | GRGDSPAS | 3JCNI5 | GRGDFSFL |
| **3JCAV1** | GRGDWTEH | 3JCLI1 | SRGDVVPP |
| **3JCAV2** | ARGDWVEG | 3JCLI2 | TRGDPPPH |
| **3JCAV3** | PRGDWTEG | 3JCLI3 | SRGDVVPP |
| 3JCAV4 | GRGDAFSL | **3JCLI4** | PRGDWNEG |
| 3JCAV5 | FRGDSPLD | **3JCLI5** | FRGDWIEL |

**Figure 1.** Phage display screening of JCFN-RGD library. M13 phage displaying a library of FNfn10 clones with partially randomized FG loops (XRGDXXXX) were amplified using 0.0 mM, 0.1 mM, or 1 mM IPTG to vary FNfn10 copy number on the phage. Amplified phage populations were subjected to three rounds of biopanning against wells coated with αvβ3 integrin (5 μg/ml). (a) A schematic drawing of FNfn10[5] showing the RGD sequence and the positions of residues in the FG loop that were diversified in the JCFNRGD library. The Figure was made with the program MOLSCRIPT.[39] (b) Five clones each were sequenced from the second round eluate of the library amplified with 1 mM IPTG (2JCAV1-2JCAV5), from the third round eluate of the library amplified with 1 mM IPTG (3JCAV1-5), from the third round eluate of the library amplified with low IPTG (3JCLI1-5), and from the third round eluate of the library amplified with no IPTG (3JCNI1-5).

eight contained an RGDWXE consensus sequence (Figure 1(b)). Phage inputs of $10^9$, $10^8$ or $10^7$ plaque-forming units (pfu) were then allowed to bind to αvβ3 or BSA-coated wells and bound phages were recovered with 0.2 M glycine (pH2.2). Using phage clones amplified in 1 mM IPTG (high FNfn10 copy number), phage clones containing the RGDWXE consensus were recovered at levels of 0.01–1% input from αvβ3-coated wells; the clones were recovered at approximately 1000-fold lower levels from BSA-coated wells and integrin-binding was found to be calcium-dependent (not shown). In contrast, clones that lacked the RGDWXE motif were recovered at equivalent levels from both αvβ3-coated and BSA-coated wells (data not shown).

The RGDWXE-containing clones were amplified in the absence of IPTG so as to decrease the expressed copy number of FNfn10 protein on the phage surface, and the panel of clones were then directly compared in a phage-binding assay, for their ability to bind to αvβ3 (not shown). The clones recovered at the highest level were 2JCAV1, 2JCAV2, 3JCAV3, 3JCNI1, and 3JCLI4, all of which were recovered at a level of approximately 0.1% of input phage from αvβ3-coated wells and at 1000-fold lower levels from BSA-coated wells. Therefore, varying FNfn10 copy number on M13 by IPTG concentration did not have an effect on the relative-binding efficiency of the clones isolated, suggesting that the binding interaction between the αvβ3 integrin and the phage-displayed FNfn10 derivatives might be of high affinity.

The modified FNfn10 proteins expressed by this panel of phage clones were expressed as isolated proteins in *Escherichia coli*, purified and biotinylated. 3JCLI4 (the second-highest recovered clone in phage-binding assays), was selected for further study because the purified FNfn10 protein derived from clone 2JCAV1 (the highest recovered clone) proved to be rather insoluble and prone to precipitation. SDS-polyacrylamide gel electrophoresis and Coomassie blue staining revealed the presence of a single protein of the expected size (~15 kDa) within the purified preparation of biotinylated FNfn10-3JCLI4 protein. Western blot analysis using a monoclonal antibody specific for the hexahistidine epitope tag on the purified FNfn10 protein confirmed the identity of this protein (not shown), and further analysis revealed that (as expected) the binding of both the phage clone 3JCLI4 and of the corresponding purified protein (FNfn10-3JCLI4) to αvβ3 integrin was $Ca^{2+}$-dependent and could be eliminated in the presence of EDTA (data not shown).

### FNfn10-3JCLI4 displays high affinity and specificity for plate-immobilized αvβ3

Biotinylated FNfn10-3JCLI4 and biotinylated wild-type FNfn10 (FNfn10-WT) were allowed to bind to αvβ3, α1β1, or BSA-coated wells in half-log increments from 0.0001 μg/ml to 0.1 μg/ml, corresponding to molar concentrations of 8 pM to 8 nM. Bound biotinylated protein was detected by ELISA (Figure 2(a)). Assuming a high ratio of free to bound FNfn10-3JCLI4, the equation $y = m1x/(m2 + x)$ was fit to the data ($R > 0.99$) to determine the half-maximal binding affinity of

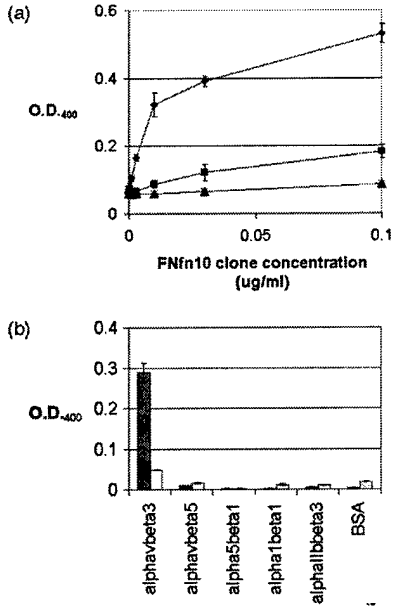


**Figure 2.** Assessment of FNfn10-3JCLI4-binding affinity to αvβ3 integrin by ELISA. (a) To determine the half-maximal binding concentration of biotinylated FNfn10-3JCLI4 *versus* biotinylated FNfn10-WT, wells of a 96-well plate were coated with αvβ3 (5 μg/ml), α1β1 (5 μg/ml), or BSA (0.5 mg/ml) and blocked with BSA. Biotinylated FNfn10-3JCLI4 and FNfn10-WT were then added to the wells and allowed to bind for two hours. Bound protein was detected by streptavidin-horseradish peroxidase (2 μg/ml) and ABTS substrate. $A_{400}$ measurements were recorded for biotinylated FNfn10-3JCLI4 binding to αvβ3 (◆) to α1β1 (▲), or to BSA (×) and biotinylated FNfn10-WT binding to αvβ3 (■). Error bars reflect the standard deviation between triplicate wells. (b) A 96-well plate was coated with αvβ3, αvβ5, αIIbβ3, α1β1, and α5β1 purified integrins, all at 5 μg/ml. Biotinylated FNfn10-3JCLI4 (dark bars) or FNfn10-WT (light bars) was then added at a concentration of 0.01 μg/ml, and allowed to incubate for two hours, followed by washing and detection. Error bars reflect the standard deviation between triplicate wells. (a) and (b) The experiments shown are all representative of three different experiments that yielded similar results.

0.01 μg/ml or 800 pM. At each concentration examined, the binding of biotinylated FNfn10-3JCLI4 to αvβ3 was higher than that for FNfn10-WT, and FNf n10-3JCLI4 was not found to bind detectably to the α1β1 integrin (i.e. binding to α1β1 was identical to binding to BSA).

To test the specificity of the interaction between FNfn10-3JCLI4 and αvβ3 integrin, biotinylated FNfn10-3JCLI4 or FNfn10-WT were added to wells coated with 5 μg/ml concentrations of different purified integrins (Figure 2(b)). In this assay, the detection of plate-bound FNfn10-3JCLI4 was significant only for those wells that had been coated with αvβ3, and not for wells coated with other integrins, including αvβ5, α5β1, α1β1 and αIIbβ3.

### The disintegrin echistatin and FNfn10-3JCLI4, but not GRGDSPK peptide or FNfn10-WT, effectively compete with biotinylated FNfn10-3JCLI4 for αvβ3 binding

In order to examine the relative affinity of FNfn10-3JCLI4 compared to other αvβ3 binding molecules, a competition ELISA analysis was performed. In these experiments, biotinylated FNfn10-3JCLI4 at 800 pM was mixed with molar ratios of competitor proteins ranging from 0.01 to 100, and allowed to bind to αvβ3-coated wells (Figure 3(a) and (b)). Binding of biotinylated FNfn10-3JCLI4 to αvβ3 was unaffected by the presence of the linear integrin-binding peptide (GRGDSPK) or FNfn10-WT, even when these molecules were added at 100-fold molar excess (80 nM) relative to FNfn10-3JCLI4. Similarly, the linear peptides PRGDWNEG and PRGDANAG also failed to inhibit FNfn10-3JCLI4 binding to αvβ3 at these same concentrations (data not shown). In contrast, unlabelled FNfn10-3JCLI4 and echistatin inhibited binding of biotinylated FNfn10-3JCLI4 at roughly equimolar concentrations ($IC_{50}$ values were 750 pM and 930 pM, respectively, as calculated by logarithmic curve-fit). These findings strongly suggest that FNfn10-3JCLI4 and echistatin have nearly equivalent affinities for αvβ3 and bind to the same site; echistatin has a published $K_d$ of 330 pM.[19]

### Alanine substitution for W or E in the RGDWXE consensus sequence reduces the affinity of FNfn10-3JCLI4 for αvβ3 integrin

In order to examine the relative affinity of FNfn10-3JCLI4 compared to mutants containing an PRGDANEG or PRGDWNAG FG loop, a competition ELISA analysis was performed. In this experiment, biotinylated FNfn10-3JCLI4 at 800 pM was mixed with molar ratios of competitor proteins ranging from 0.01 to 100, and allowed to bind to αvβ3-coated wells (Figure 3(c)). Both FNfn10-3JCLI4(RGDANE) and FNfn10-3JCLI4(RGDWNA) showed reduced ability to compete with biotinylated FNfn10-3JCLI4 compared to unlabelled, unmodified FNfn10-3JCLI4.

### FNfn10-3JCLI4 is an effective and specific staining reagent, when used in flow cytometric analysis

Biotinylated FNfn10-3JCLI4 (1 μg/ml) was added to wild-type K562 cells (α5β1-positive) and to K562 cells that had been stably transfected with αvβ3 integrin (generous gift from Dr S. Blystone).[20] Surface-bound FNfn10-3JCLI4 was then detected using streptavidin-APC and stained cells were enumerated by flow cytometry. The mean fluorescence intensity of staining on the αvβ3-positive cells was approximately three logs higher than on the non-transfected control cells (Figure 4(a)), and concentrations of biotinylated FNfn10-3JCLI4 as

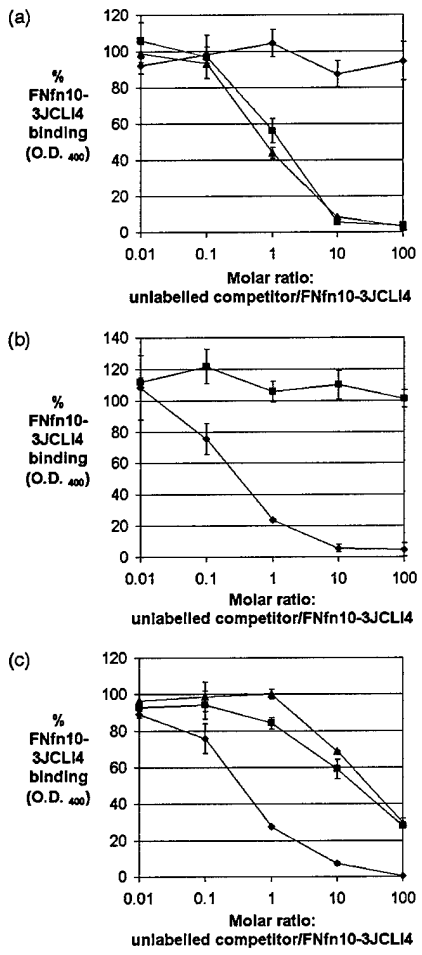


**Figure 3.** Competition ELISAs to determine relative affinities of FNfn10-3JCLI4, echistatin, FNfn10-WT, and GRGDSPK peptide. A BSA-blocked 96-well plate was coated with αvβ3 at 5 μg/ml, and biotinylated FNfn10-3JCLI4 was then added in the presence or absence of a 0.01, 0.1, 1, 10, or 100-fold molar excess of unlabelled competitor protein, and incubated for two hours. After washing and detection, the $A_{400}$ of the plate was recorded. Error bars reflect the standard deviation between triplicate wells, and the results shown are representative of three different experiments that yielded similar results. A background subtraction was performed on all data points, by subtracting the measured $A_{400}$ value that corresponded to binding of biotinyated FNfn10-3JCLI4 in the presence of 10 mM EDTA. All values in the Figure are expressed as a percentage of the $A_{400}$ of biotinylated FNfn10-3JCLI4 binding in the absence of competitor. (a) Binding competition with unlabelled FNfn10-3JCLI4 (▲), echistatin (■), and GRGDSPK peptide (◆). (b) Binding competition with unlabelled FNfn10-3JCLI4 (◆) or unlabelled FNfn10-WT (■). (c) Binding competition with unlabelled FNfn10-3JCLI4 (◆), unlabelled FNfn10-3JCLI4(RGDANE) (■), and unlabelled FNfn10-3JCLI4(RGDWNA) (▲).

low as 8 ng/ml were found to be capable of effectively and specifically staining K562-αvβ3 cells (data not shown).

Having optimized our staining analysis using the K562-αvβ3 cells, we proceeded to a more complete analysis of the specificity of cell surface binding of biotinylated FNfn10-3JCLI4, using a panel of K562 cell sublines, each of which had been stably transfected with various integrin heterodimers (αvβ3, αvβ5, αIIbβ3, α4β1, and α4β7; gift from S. Blystone).[20] These experiments revealed that FNfn10-3JCLI4 showed a strong selective preference for αvβ3, although it did also react very weakly with αIIbβ3 positive cells. In contrast, FNfn10-WT showed a slight preference for cells expressing αvβ3, but stained all of the K562 lines with low intensity (Figure 4(b)).

One of the unique properties of the FNfn10 scaffold is its high level of physical stability. We therefore examined the effect of prolonged incubation at elevated temperatures on the binding activity of FNfn10-3JCLI4, as compared to the αvβ3-specific monoclonal antibody, LM609. In these studies, FNfn10-3JCLI4 and LM609 were incubated for 24 hours at 4 °C, 20 °C, 37 °C, 50 °C, 65 °C, or 75 °C, prior to addition to K562-αvβ3 cells and performance of flow cytometry. As can be observed in Figure 4(c), incubation of biotinylated FNfn10-3JCLI4 at 75 °C for 24 hours had only a modest effect on its cell-binding activity; in contrast, the same conditions resulted in the complete elimination of LM609's ability to interact with αvβ3.

### FNfn10-3JCLI4 inhibits αvβ3-dependent cell adhesion but not αIIbβ3-dependent cell adhesion

K562-αvβ3 cells, but not K562 cells (α5β1-positive), adhere strongly to vitronectin (but not BSA). This property was therefore used as the basis for a quantitative assessment of the ability of FNfn10-3JLCI4 to disrupt αvβ3-dependent cell adhesion. To do this, K562-αvβ3 cells were allowed to adhere to vitronectin-coated wells, and the number of bound cells per well was then quantified by crystal violet staining and cell solubilization.

LM609, a commonly used αvβ3 function-blocking antibody, and FNfn10-3JCLI4 were both found to inhibit adhesion of K562-αvβ3 cells to vitronectin, while FNfn10-WT showed little effect in this assay (Figure 5(a)). A more careful analysis, using a wider range of protein concentrations, revealed that FNfn10-3JCLI4 inhibits αvβ3-dependent adhesion to vitronectin at approximately the same concentrations as the well-characterized, αvβ3-binding disintegrin, echistatin (Figure 5(b)). Based on an exponential curve-fit, echistatin was found to inhibit αvβ3-mediated cell adhesion to vitronectin with an $IC_{50}$ of 5.9 nM, while FNfn10-3JCLI4 inhibited αvβ3-dependent adhesion to vitronectin with an $IC_{50}$ of 8.6 nM ($R > 0.99$ in both cases). We also examined the effect of

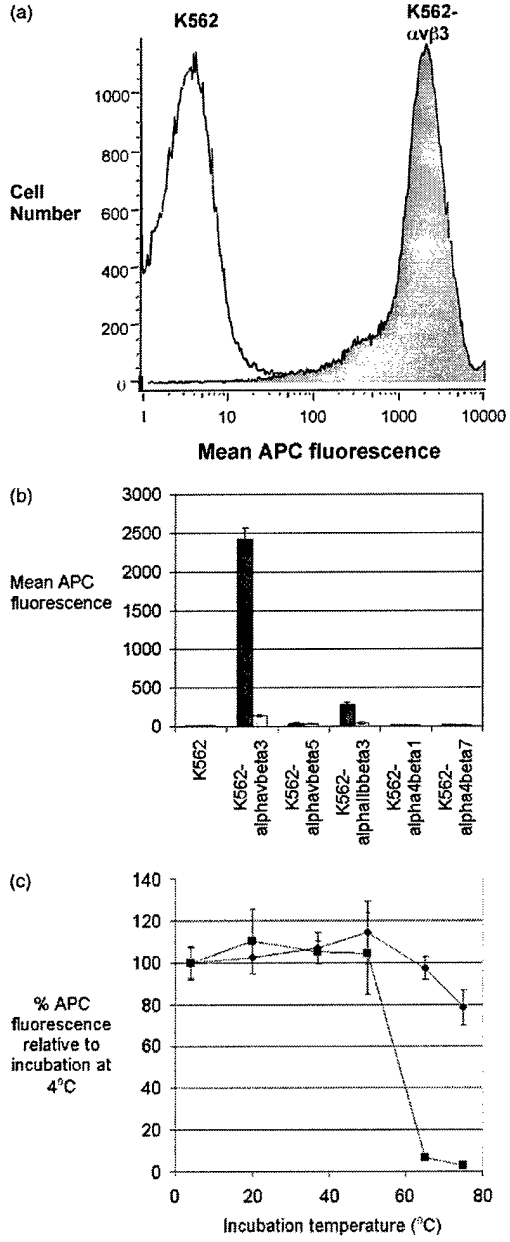


**Figure 4.** Flow cytometric analysis of FNfn10-3JCLI4 binding to human cells. Biotinylated FNfn10-3JCLI4 or FNfn10-WT were added to $10^5$ cells at a concentration of 1 μg/ml and incubated for 30 minutes. Bound proteins were then detected with streptavidin-APC, and the mean fluorescence of 10,000 cells per sample was recorded. All experiments were performed three times, with similar results; error bars (b and c) represent the standard deviation of three samples of $10^5$ cells stained separately. (a) Histogram plot of flow cytometric staining analysis of K562 and K562-αvβ3 cells using FNfn10-3JCLI4. (b) Mean APC fluorescence for integrin-transfected K562 cells stained with biotinylated FNfn10-3JCLI4 (dark bars) or FNfn10-WT (light bars). (c) To determine the effect of high temperature on FNfn10-3JCLI4 stability, 1 μg /ml FNfn10-3JCLI4 (◆) or 5 μg/ml LM609 (■) were incubated for 24 hours in FACS buffer at 4 °C, 20 °C, 37 °C, 50 °C, 65 °C, or 75 °C. $10^5$ K562-αvβ3 cells were pelleted for each sample and resuspended in the appropriately treated FNfn10-3JCLI4 or LM609, followed by detection as above. Results (mean fluorescence) are expressed as a percentage of values determined after FNfn10-3JCLI4 or LM609 were incubated at 4 °C prior to their addition to the cells.

FNfn10-3JCLI4 on αIIbβ3-dependent cell adhesion, because of the weak-binding activity of FNfn10-3JCLI4 for K562-αIIbβ3 cells that was revealed in our flow cytometric analyses. These experiments revealed that FNfn10-3JCLI4 inhibited αIIbβ3-mediated cell adhesion to vitronectin at concentrations between one and two logs higher than the inhibitory concentrations of echistatin. Estimated $IC_{50}$ values based on logarithmic curve fit were approximately 150 nM for FNfn10-3JCLI4 (two points only, no $R$ value calculated) and 6.3 nM for echistatin ($R > 0.99$) (Figure 5(c)). Non-transfected K562 cells (α5β1-positive) adhered strongly to fibronectin and while FNfn10-3JCLI4 showed no discernable inhibition at concentration up to 400 nM, echistatin inhibited adherence of K562 cells to fibronectin with an approximate $IC_{50}$ of 56 nM ($R > 0.99$) (Figure 5(d)).

### Alanine substitution for W or E in the RGDWXE consensus sequence reduces the specificity of FNfn10-3JCLI4 for αvβ3 integrin in cell adhesion assays

Table 1 shows the relative inhibition of K562 lines by FNfn10-3JCLI4, FNfn10-3JCLI4(RGDANE), or FNfn10-3JCLI4(RGDWNA). These experiments were performed in the presence of 160 nM inhibitor, well above the concentration of FNfn10-3JCLI4 required to completely inhibit adhesion of K562-αvβ3 cells to vitronectin, in order to identify the cross-reactivities of the alanine substitution mutants, known to bind αvβ3 integrin with lower affinity. These experiments show that while FNfn10-3JCLI4 and FNfn10-3JCLI4(RGDANE) show virtually no cross-reactivity with αvβ5 integrin at this concentration, FNfn10-3JCLI4(RGDWNA) shows nearly half-maximal inhibition. As expected, FNfn10-3JCLI4 shows cross-reactivity with αIIbβ3 at this concentration; FNfn10-3JCLI4(RGDANE) also cross-reacts at near half-maximal affinity while FNfn10(RGDWNA) shows somewhat less cross-reactivity. Therefore, it appears that the tryptophan in the RGDWXE consensus sequence may be more important in conferring specificity to αv over αIIb, while the glutamic acid residue may confer specificity to β3 over β5.

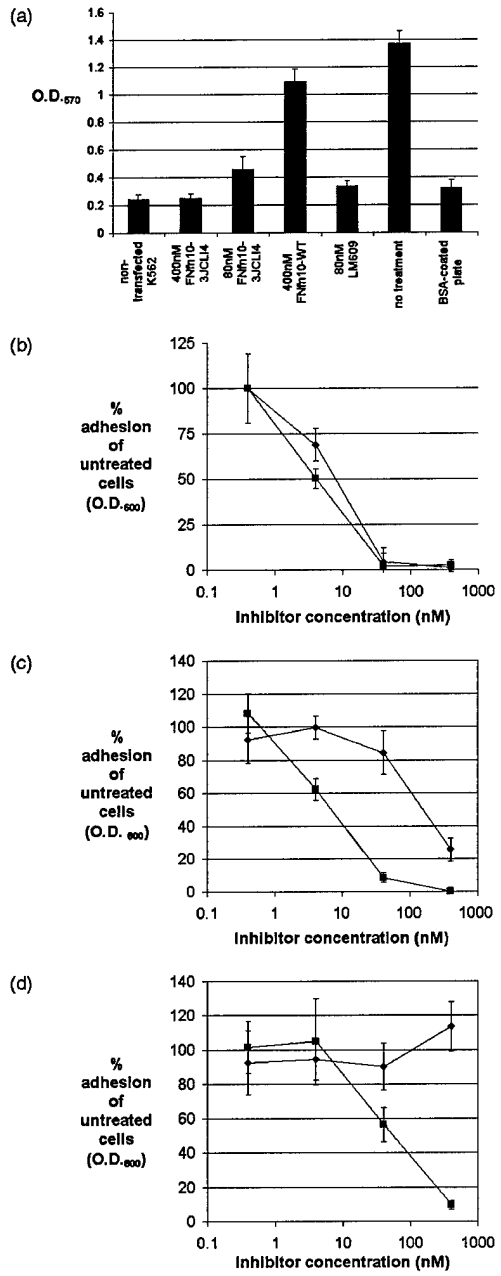


**Figure 5.** Inhibition of integrin-dependent cell adhesion. Vitronectin (a–c) or fibronectin (d) coated strips (as well as uncoated control wells) were incubated with $10^5$ K562 cells, K562-αvβ3 cells, or K562-αIIbβ3 cells for two hours in the presence or absence of the indicated inhibitors. Non-adherent cells were removed by washing, while adherent cells were stained with crystal violet, solubilized, and quantified by measuring the $A_{600}$. The background level of crystal violet in control wells was calculated on the basis of measured $A_{600}$ for BSA-coated wells (no integrin). Error bars represent the standard deviation of triplicate wells, and all experiments were performed three times, with similar results. (a) Adhesion of K562-αvβ3 cells to vitronectin. Inhibitors added include FNfn10-3JCLI4, FNfn10-WT, and LM609 antibody, at the stated final concentrations. The lane marked "non-transfected K562" corresponds to control K562 cells (no αvβ3), while "BSA coated plate" denotes cell adherence (K562-αvβ3 cells) measured on control wells (no vitronectin); the lane marked "no treatment" corresponds to K562-αvβ3 cells which were bound to vitronectin in the absence of any competitor. (b) Adhesion of K562-αvβ3 cells to vitronectin. Echistatin (■) and FNfn10-3JCLI4 (◆) were added at final concentrations of 400 nM, 40 nM, and 4 nM, prior to addition of the cells and initiation of the binding assay. Binding is expressed as a percentage of the $A_{600}$ recorded for K562-αvβ3 adhesion in the absence of competitor, and a background subtraction was performed for all data points, which corresponded to the measured $A_{600}$ for BSA-coated wells (no integrin). (c) Adhesion of K562-αIIbβ3 cells to vitronectin. Echistatin (■) and FNfn10-3JCLI4 (◆) were added at final concentrations of 400 nM, 40 nM, and 4 nM prior to addition of the cells and initiation of the binding assay. Binding is expressed as a percentage of the $A_{600}$ recorded for K562-αIIbβ3 adhesion in the absence of competitor, and a background subtraction was performed for all data points, which corresponded to the measured $A_{600}$ for BSA-coated wells (no integrin). (d) Adhesion of K562 cells to fibronectin. Echistatin (■) and FNfn10-3JCLI4 (◆) were added at final concentrations of 400 nM, 40 nM, and 4 nM prior to addition of the cells and initiation of the binding assay. Binding is expressed as a percentage of the $A_{600}$ recorded for K562 adhesion in the absence of competitor, and a background subtraction was performed for all data points, which corresponded to the measured $A_{600}$ for BSA-coated wells (no integrin).

**Table 1.** Inhibition of integrin dependent cell adhesion by alanine substitution FNfn10-3JCLI4 mutants

| | K562-αVβ3 | K562-αVβ5 | K562-αIIbβ3 |
|---|---|---|---|
| 3JCLI4 | 99.2 ± 1.3 | 0.0 ± 3.8 | 67.8 ± 2.9 |
| 3JCLI4-RGDANE | 21.7 ± 5.2 | 1.7 ± 8.1 | 43.2 ± 4.0 |
| 3JCLI4-RGDWNA | 40.5 ± 7.3 | 41.6 ± 2.5 | 17.9 ± 5.8 |
| Anti-αVβ3 mAb | 84.0 ± 7.5 | | |

Chart values reflect the percentage inhibition (100% − % background-subtracted $A_{600}$ for K562 line adhesion to vitronectin in the absence of competitor, background subtraction as in Figure 5) plus/minus the standard deviation of triplicate wells. A value of 100% corresponds to a complete absence of cell adhesion to the well. All experiments were performed three times in a manner identical to the experiments described in the legend to Figure 5, with similar results. All inhibitors were added at a concentration of 160 nM, well above the concentration required for complete inhibition of K562–αvβ3 cells by FNfn10-3JCLI4.

## FNfn10-3JCLI4 interferes with *in vitro* endothelial capillary tube formation

Using the Quantimatrix (Chemicon) *in vitro* extracellular membrane system, SV-HCECs spontaneously formed capillary tubes within three to five hours and this process was stimulated by the presence of bFGF. Both LM609 anti-αvβ3 mAb (20 μg/ml) and FNfn10-3JCLI4 (0.1 μg/ml), but

not FNfn10 (0.1 μg/ml), inhibited this process as assessed by total tube length per center field and by total number of tubes per well (Figure 6(a) and (b)). LM609 did not consistently inhibit tube formation at lower concentrations (data not shown).

## Discussion

Here, we have applied phage display technology and random mutagenesis techniques to carry out affinity maturation of FNfn10 binding to αvβ3 integrin. Using one phage clone that was derived from a biopanning screen against immobilized αvβ3, 3JCLI4, we found the following: (i) modified FNfn10 phage clones, including 3JCLI4, which bind to αvβ3 integrin, all contain a RGDWXE consensus; (ii) purified FNfn10-3JCLI4 protein binds to immobilized human αvβ3 integrin with much higher affinity than FNfn10-WT and exhibits only background binding to other purified integrins; (iii) binding of FNfn10-3JLCI4 to αvβ3 could be successfully competed using approximately equimolar concentrations of unlabelled FNfn10-3JCLI4 or echistatin, but not by either FNfn10-WT or GRGDSPK peptide (even when added at 100-fold molar excess); (iv) FNfn10-3JCLI4 is a sensitive and specific reagent for the detection of human αvβ3 integrin in flow cytometry applications; (v) the binding of FNfn10-3JCLI4 to αvβ3 integrin is maintained even after prolonged exposure of FNfn10-3JCLI4 to high temperature; (vi) FNfn10-3JCLI4 inhibits cell adhesion to vitronectin *via* αvβ3 at much lower (nanomolar) concentrations than it inhibits cell adhesion to vitronectin *via* αIIbβ3 in transfected K562 cells; (vii) replacement of the W or E in the PRGDWNEG FG loop sequence on FNfn10-3JCLI4 reduces both the affinity and specificity of αvβ3 interactions; and (viii) FNfn10-3JCLI4 inhibits *in vitro* endothelial capillary tube formation.

The RGDW consensus sequence that was detected in our αvβ3-selected FNfn10-display phage clones has previously been reported to be preferentially selective for αIIbβ3 integrin over αvβ3, at least in the context of disintegrins such as eristostatin.[21] RGDW peptides are also used to induce integrin activation and in competition assays with putative αIIbβ3 integrin ligands.[22] Because FNfn10-3JCLI4 exhibits no binding to plate-immobilized αIIbβ3 and very low cross-reactivity with αIIbβ3-positive cells in flow cytometric analyis and cell adhesion assays, the tertiary structure of FNfn10 may play a role in the increased specificity of this RGDW-containing molecule for αvβ3 integrin. Alternatively, the glutamic acid residue within the extended consensus motif (RGDWXE) may be significant. The disintegrins eristostatin and EC6B each contain an aspartic acid residue at the corresponding location (RGDWND),[21,23,24] and though they both bind αvβ3, they interact preferentially with αIIbβ3. In our studies with alanine substitution mutants of

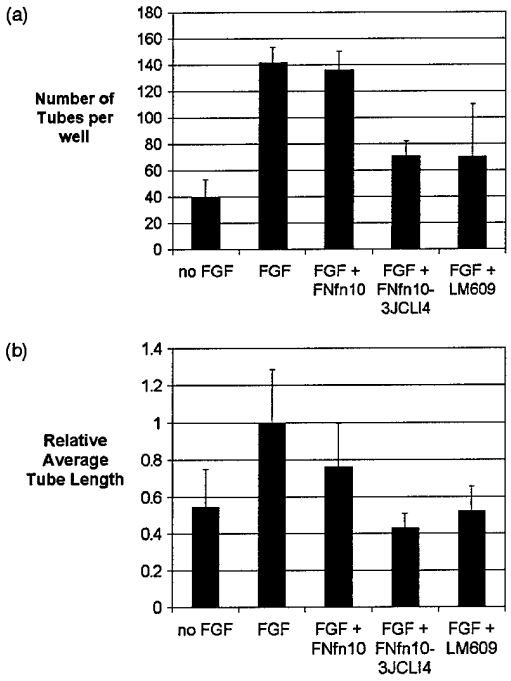


**Figure 6.** Inhibition of *in vitro* capillary tube formation by FNfn10-3JCLI4. SV40-immortalized human cerebral endothelial cells (SV-HCECs) were incubated on Quantimatrix in the presence or absence of inhibitor for three to five hours at 37 °C until capillary tube formation was observed. At that time, the total number of tubes per well (96-well plate) were counted by a blinded observer as described in Experimental Procedures (Figure 6(a)). Alternatively, the total relative tube length was measured for the center field of a 24-well plate as described in Experimental Procedures (Figure 6(b)). Error bars represent the standard deviation of triplicate wells, and both experiments were performed three times, with similar results.

FNfn10-3JCLI4, both the tryptophan and glutamic acid residues are necessary for maximal binding affinity. In results contradictory to the known disintegrin and other RGDW sequence data, it appears that loss of the tryptophan residue in the RGDWXE consensus sequence confers greater cross- reactivity to αIIbβ3 integrin and that loss of the glutamic acid residue confers greater cross-reactivity to αvβ5 integrin. These differences may be due to the shorter, more constrained loop structure of FNfn10 compared to disintegrins. It will be interesting to characterize the three-dimensional structure and conformational dynamics of the FNfn10 mutants obtained in this study.

Like the disintegrins, FNfn10-3JCLI4 is a small monomeric molecule with high integrin-binding affinity. In our studies, echistatin and FNfn10-3JCLI4 were inferred to have similar binding affinities for αvβ3 because they were both able to compete with biotinylated FNfn10-3JCLI4 for

binding to immobilized αvβ3, at roughly equimolar concentrations. Consistent with this, echistatin has a reported $K_d$ of 330 pM for αvβ3[19] while the value calculated here for the half-maximal binding affinity of FNfn10-3JCLI4 for αvβ3 was 800 pM.

This affinity is considerably higher than the measured binding affinities of other integrin-ligands that have been isolated *via* phage display technology, including conventionally derived cysteine-constrained peptides, which have at best yielded molecules with a high nanomolar binding affinity for their target integrin.[4,25,26] In general, these cyclic peptides also exhibit a lesser degree of selectivity for the specific integrin against which they were selected, as compared to the FNfn10-3JCLI4. Available data on the αvβ3-binding proteins selected using the CTLA-4 scaffold do not include information pertaining to protein binding affinities or integrin selectivity,[18] so it is difficult to make direct comparisons to the present work. However, more directed protein engineering approaches have resulted in results analogous to these described here. For example, the "grafting" of the complementarity-determining region of a αIIbβ3-specific monoclonal antibody onto a surface loop within the tissue plasminogen activator protein resulted in the creation of a hybrid protein with a binding affinity for αIIbβ3 of 900 pM.[27] Disadvantages of this grafting approach include the fact that it requires that one have in-hand a monoclonal antibody or similar reagent, and that the binding specificity/affinity conferred by this reagent should not be destroyed when it is placed in a novel context.

One other approach to the derivation of novel integrin-binding proteins was described recently by Tani and colleagues.[28] These workers performed directed protein evolution (mutagenesis, followed by phage display and selection) of the ninth and tenth domains of fibronection,[28] and they identified a mutant (D1418V) that possessed enhanced (low nanomolar) binding to the integrins αIIbβ3 and α5β1, but not αvβ3. Interestingly, this residue is located in the linker region between the FN9 and Fn10 domains, well away from either the RGD or the MIDAS motif.[28]

In any event, the high affinity of FNfn10-3JCLI4 for αvβ3, suggested that FNfn10-3JCLI4 might be suitable for use in flow cytometric applications. Experimental analysis revealed this was indeed the case, and these studies also showed that FNfn10-3JCLI4 performed with similar specificity to an αvβ3-specific monoclonal antibody in flow cytometric staining using K562-αvβ3 cells. It should be noted that FNfn10-3JCLI4 is monomeric, unlike monoclonal antibodies (divalent) or other cell-staining reagents used in flow cytometry (MHC:peptide tetramers). Furthermore, FNfn10-3JCLI4 is considerably more heat stable than a typical monoclonal antibody, as revealed by its ability to continue to bind αvβ3, even after 24 hours incubation at 75 °C.

A problem encountered in many molecules that target αvβ3 integrins is their cross-reactivity with other integrin subtypes, particularly other αv or β3 integrins. FNfn10-3JCLI4 was found to bind only to immobilized purified αvβ3, and not to other integrins tested. The failure of FNfn10-WT and FNfn10-3JCLI4 to interact with α5β1 is consistent with previous reports that the ninth and eighth fibronectin type III domains are also required for FNfn10 binding to α5β1.[29] In addition, the inability of FNfn10-3JCLI4 to bind to αvβ5 and αIIbβ3 suggests that its integrin-binding activity is likely dependent on a structural interaction with the αvβ3 complex and not with either subunit alone. The narrow integrin-binding specificity of FNfn10-3JCLI4 can be contrasted with the more broad integrin-binding profile that is exhibited by disintegrins such as eristostatin and kistrin, which bind to both αIIbβ3 and αvβ3.[21] Similarly, the penton base protein from adenovirus type 5 binds to both αvβ3 and αvβ5, and the engineered Fab construct (WOW-1) exhibits cross-reactivity with αvβ5 integrin similar to that of penton base.[30]

The FG loop of FNfn10 that contains the RGD sequence is highly dynamic and it is disordered in the X-ray and NMR structures.[5,31] Thus, these structures do not provide a reliable template to model the FG loop of 3JCLI4 or to perform a docking study using the crystal structure of αvβ3.[32,33] However, a close examination of the αvβ3 structure provided insights into the potential mechanism of the increased affinity and specificity of 3JCLI4 toward αvβ3.

In the crystal structure of αvβ3 in complex with an RGD peptide,[33] the residue following the Asp of the peptide (D-Phe in this crystal structure) is highly exposed, suggesting that the Trp residue in the RGDWXE motif would be readily accommodated in this binding pocket. Moreover, there is a small hydrophobic pocket near this Phe side-chain. Thus, it is possible that binding of the Trp side-chain into this pocket is responsible for the enhanced affinity of 3JCLI4 to αvβ3.

There are three Mn cations in the vicinity of the RGD-binding site of αvβ3 in the αvβ3-RGD complex. The Asp side-chain carboxylate group of the RGD peptide contacts a Mn cation at the so-called MIDAS (metal ion-dependent adhesion site). Another Mn cation at the so-called AMIDAS (adjacent to MIDAS) is primarily coordinated by Asp126 and Asp127 of β3. This cation is located at a position that could be reached by the carboxylate group of Glu in the RGDWXE motif. A Ca cation was found at the AMIDAS in the unliganded structure of αvβ3 that was determined in the presence of Ca.[32] Thus, it is highly likely that a Ca cation at the AMIDAS was present in our screening, which was also performed in the presence of Ca.

The Glu to Ala mutation in the RGDWXE motif resulted in a significant increase in the inhibition of αvβ5-mediated cell attachment (Table 1). This

suggests increased affinity of the mutant (3JCLI4-RGDWNA) to αvβ5. Although residues at the MIDAS and AMIDAS are nearly completely conserved between the β3 and β5 integrins, Trp129 of β3 is replaced with Asp in β5.[34] It is tempting to speculate that 3JCLI4 probes a difference in the conformation at or near the AMIDAS and that the Glu-to-Ala mutation abolishes the ability of 3JCLI4 to discriminate the conformational difference at this location.

3JCLI4 does not bind well to αIIbβ3, suggesting that 3JCLI4 can discriminate the αIIb from αv. In the αvβ3-RGD complex, only the Arg residue of the RGD peptide makes extensive interactions with the αv subunit. Two residues that make direct contacts with the Arg side-chain are different between αv and αIIb (Ala215 and Asp218 in αv *versus* Glu and a deletion, respectively, in αIIb), suggesting that the property of the Arg-binding site may be significantly different between these two α subunits. It is also possible that the FG loop of 3JCLI4 makes additional contacts with the α subunit, which may enhance the binding specificity.

FNfn10-3JCLI4 did exhibit a weak interaction with αIIbβ3 in our flow cytometry assay, but we do not anticipate that this will be a major detriment to the more widespread use of this molecule in cell staining applications because (i) no interaction with αIIbβ3 was detected in biochemical binding studies (see above), (ii) binding to αIIbβ3 positive cells was almost tenfold weaker than binding to αvβ3-positive cells in the flow cytometric analysis, and (iii) αIIbβ3 expression is limited to platelets. The ability of FNfn10-3JCLI4 to block αvβ3-dependent cell adhesion at similar concentrations to echistatin, its lack of cross-reactivity with α5β1 in inhibition of cell adhesion to vitronectin, and its low inhibition of αIIbβ3-dependent adhesion to vitronectin compared to echistatin further supports its specifity for αvβ3. The cross-reactivity to αIIbβ3 observed in cell adhesion assays was similar to that of a monoclonal antibody known to be specific for αvβ3, so it may be due to generally weak interactions of αIIbβ3 with vitronectin in this system. Slight cross-reactivity (1–10%) of FNfn10-3JCLI4 with αIIbβ3 is also not expected to be a problem in gene delivery applications, since platelets are anucleate and thus lack transcriptional machinery.

The structure of FNfn10-3JCLI4 is advantageous for multiple applications; FNfn10-3JCLI4 lacks disulfide bonds, rendering it resistant against reducing agents, is very stable even at high temperature, and can be produced in a bacterial expression system with yields of up to 50–100 mg per liter of culture. Since FNfn10-3JCLI4 is a monomer that lacks disulfide bonds, it has several advantages over a monoclonal antibody with similar affinity. As a small, single-chain molecule, FNfn10-3JCLI4 could potentially be incorporated into gene delivery vectors (e.g. viral vectors, liposomes) for cell or tissue-specific gene expression. Indeed, the incorporation of low-affinity RGD peptides into various viral vectors, and the addition of bispecific antibody complexes to viral surface components, have already been shown to result in desirable improvements in vector specificity and transduction efficiency.[35–38] αvβ3-positive cells that may be of particular interest for targeted vector systems include dendritic cells (for vaccine applications) as well as osteoclasts and angiogenic vessels. Finally, FNfn10-3JCLI4 may have utility as a cancer imaging agent, because of its ability to recognize αvβ3 on tumor vasculature, which is supported by its *in vitro* inhibition of capillary tube formation. Further studies will be required to explore these various applications.

## Experimental Procedures

### General reagents

All chemicals, unless otherwise specified, were obtained from Sigma (St. Louis, MO). Purified integrins, cell adhesion strips, and LM609 were purchased from Chemicon (Temecula, California). Echistatin and GRGDSPK peptide were obtained from Bachem (Torrence, California).

### Cell culture

K562, K562-αvβ3, K562-αIIbβ3, K562-αvβ5, K562-α4β1, and K562-α4β7 cells were a gift from Dr S. Blystone (Upstate Medical University, Syracuse, NY);[20] expression of integrins was confirmed by flow cytometry. K562 cells were maintained in Iscove's Modified Dulbecco's Medium (IMDM) (Gibco, Invitrogen, Grand Island, NY) supplemented with 10% (v/v) fetal bovine serum (Sigma), 0.5 unit/l penicillin-streptomycin, and 2 mM L-glutamine (Gibco). K562-αvβ3, K562-αIIbβ3, K562-αvβ5, K562-α4β1, and K562-α4β7 cells were maintained in the same media containing 500 μg/ml G418 (Geneticin) (Gibco). SV40-immortalized human cerebral endothelial cells (SV-HCECs, gift from D.B. Stanimirovic, University of Montreal) were maintained in RPMI 1640 (Gibco) supplemented with 20% fetal bovine serum (Sigma), 0.5 unit/l penicillin-streptomycin, 2 mM L-glutamine (Gibco), 10 μg/ml heparin (Sigma), and 1 μg/ml hydrocortisone (Sigma). Some SV-HCECs, as noted, were also maintained in 10 ng/ml basic fibroblast growth factor (Gibco).

### Construction of phage vectors

We constructed a phage-display vector for FNfn10, JCFN, by cloning the FNfn10 gene[7] in the modified M13 vector, JC-M13-88.[40] The FNfn10 gene was amplified from pAS38[7] using oligonucleotides FN3JCM8Nhe (CCT AGCTAGCGTAGCTCAGGCCATGCAGGTTTCTGATG TTC) and FN3JCM8Hin (GGCCAAGCTTGACCGCCAC CAGAACCGCCACCGGTACGGTAG), digested with the restriction enzymes *Nhe*I and *Hin*dIII, and subcloned in JC-M13-88 using the same restriction enzyme sites so that the FNfn10 gene is placed in-frame between the OmpA signal sequence and M13 gene VIII. We confirmed that the JCFN phages prepared using *E. coli* XL-1blue displayed FNfn10 on the phage surface by ELISA (data not shown). Purified FNfn10 clones were

expressed with an N-terminal His-tag and a C-terminal GKKGK tag. The GKKGK tag was incorporated to increase the solubility[7] and to serve as a preferred chemical modification site. FNfn10 genes were amplified using oligonucleotides FN1F2 (CGGGATCCCATATGC AGGTTTCTGATGTTCCGCGTGACCTGGAAGTT GTTGCTGCGACC) and FN3GKKGK (CCGACTCGAG TTACTATTTACCTTTTTTACCGGTACGGTAGTT AATCGAG), digested with the restriction enzymes *Nde*I and *Xho*I, and ligated with pAS45[7] digested with the same restriction enzymes. The expression vector for the wild-type protein, pAS54, contained an Arg6 to Thr mutation that had been introduced to remove a secondary Thrombin site.[7]

### Construction of the FNfn10 library

We constructed a FNfn10 library, JCFN-RGD, in such a way that the FG loop has XRGDXXXX sequence where X stands for any amino acid (residues 77–84; residue numbering is according to Figure 2(a) of Koide *et al.*[7]) Mutagenesis on the JCFN template was performed following Kunkel's method[41] using an oligonucleotide JCFNFGRGD (GTTAATCGAGATTGGCTTGGAMNNM NNMNNMNNATCGCCGCGMNNAGTAACAGCGTAT AC, where N is a mixture of A, G, C and T, and M is a mixture of A and C). *E. coli* SS320 was electro-transformed with the mutagenesis mixture, resulting in a phage library containing $1.5 \times 10^9$ independent clones. The phages were re-amplified in *E. coli* XL1-blue with various concentrations of isopropyl β-D-thiogalactopyranoside (IPTG).

### αvβ3 biopanning using the JCFN-RGD library

Integrin biopanning was performed similarly to the method described.[42] Purified αvβ3 (5 μg/ml in TBS buffer containing 2 mM $CaCl_2$) was bound to a single microtiter well of a 96-well plate. The well was rinsed three times with sterile water containing 2 mM $CaCl_2$ and blocked with 5% phage blocking reagent (Novagen, Darmstadt, Germany) for one hour at room temperature. The plate was rinsed five times with TBS buffer containing 0.1% Tween-20 and 2 mM $CaCl_2$, then incubated with JCFN-RGD library diluted in 5% blocking reagent for one hour. The plate was washed ten times with TBS buffer containing 0.1% Tween 20 and 2 mM $CaCl_2$ and bound phage were eluted with 0.2 M glycine-HCl (pH 2.2) containing 1 mg/ml BSA for ten minutes at room temperature with gentle agitation and neutralized with 15% (v/v) 1 M Tris–HCl (pH 9.1). The phage were amplified using the *E. coli* ER2738 host strain (New England Biolabs, Beverly, MA) in the presence of 1 mM, 0.1 mM or with no IPTG and purified by precipitating with 20% (w/v) polyethylene glycol-8000, 2.5 M NaCl and resuspending in PBS containing 20% (v/v) glycerol. The biopanning and amplification of eluted phage were repeated for two more rounds. Upon completion of three rounds of biopanning, individual phage clones were amplified and the genomes were purified by phenol-extraction. Polymerase chain reaction was performed with the primers SFN3F (AGCTCAATTGGTCC GGTGGAGGTTCTGATGTTCCGCGTGACCTG) and SFN3R (AGCTAAGCTTTTAGGTACGGTAGTTAATCG AGAT) to amplify the FNfn10 domain. The DNA was sequenced using the SFN3F primer.

### Construction of pET/JCLI4-W to A and pET/JCLI4-E to A plasmids

The DNA fragment which contains a tryptophan to alanine mutation in the FG loop of FNfn10-3JCLI4 was constructed using PCR. The first PCR was performed using oligonucleotides T7 promoter primer (TAATACG ACTCACTATAGGG) and JCLI4WtoAR (GGTACGGTA GTTAATCGAGATTGGCTTGGACCCCTCATTCGCATC GCCGCGAGGAGTAAC), and pET/3JCLI4 as the template. After the PCR product was purified with QIAquick PCR purification kit (Qiagen), the second PCR was performed using oligonucleotides T7 promoter primer and FNGKKGKR (CCGACTCGAGTTACTATTT ACCTT TTTTACCGGTACGGTAGTTAATCGAG), and the purified first PCR product as the template. The second PCR product was purified with QIAquick PCR purification kit, digested with XbaI and XhoI, and the DNA fragment was recovered after electrophoresis using QIAEX II gel extraction kit (Qiagen). The DNA fragment was ligated with the plasmid pAS45,[7] which was digested with XbaI and XhoI and cleaned up with QIAEX II gel extraction kit. The resulting plasmid is pET/JCLI4-W to A.

The plasmid pET/JCLI4-E to A, that has a glutamic acid to alanine mutation in the FG loop of JCLI4-FN, was constructed in the same way except that a primer JCLI4 EtoAR was used instead of JCLI4WtoAR (GGTAC GGTAGTTAATCGAGATTGGCTTGGACCCGGCATTCC AATCGCCGCGAGG).

### Protein preparation

The expression of FNfn10 proteins was performed as described[7] except that the proteins were further biotinylated. After purification, the protein-containing solution was applied to a nickel affinity column and unbound materials were washed off; the column was then equilibrated with 50 mM sodium phosphate buffer (pH 8.0) containing 500 mM sodium chloride. D-Biotinoyl-ε-aminocaptoic acid *N*-hydroxysuccinimide ester (726 μM) (Boehringer Mannheim, Mannheim, Germany) in the same buffer was applied to the column, and the column was incubated for an hour at room temperature to perform biotinylation. The column was washed with 20 mM Tris–HCl buffer (pH 8.0) containing 500 mM sodium chloride, and the biotinylated FNfn10 was eluted with the buffer containing 500 mM imidazole. The proteins purified in this manner were >90% pure as judged by SDS-PAGE and reverse phase chromatography. Protein concentrations for subsequent analyses were determined by Bradford assay and confirmed by SDS-PAGE analysis and Coomassie Brilliant Blue staining. Biotinylation was confirmed by Western analysis with streptavidin-horseradish peroxidase (Oncogene, Cambridge, MA).

### ELISA detection of biotinylated FNfn10 clones

Purified integrin was bound to a flat-bottom, high-binding EIA/RIA plate (Corning Costar, Corning, NY) at a concentration of 5 μg/ml in TBS for 12–16 hours at 4 °C. The plate was washed once with TBS and blocked for two hours at room temperature with 0.1 M $NaHCO_3$, 0.5 mg/ml BSA, 0.2% $NaN_3$ (pH 8.6). Biotinylated FNfn10 clones were bound in TBST + $Ca^{2+}$ (TBS, 0.1% Tween-20, 2 mM $CaCl_2$). Plates were washed ten times with TBST + $Ca^{2+}$ and incubated 20 minutes with 2 μg/ml streptavidin-horseradish peroxidase (Oncogene) in

TBST + $Ca^{2+}$ at room temperature. Plates were washed ten times with TBST + $Ca^{2+}$. Bound peroxidase was detected with ABTS (2,2'-azino-di-3-ethyl-benzthiazoline sulfonic acid) peroxidase substrate (Sigma), 1 mg/ml in 0.1 M sodium citrate, 0.1 M $Na_2HPO4$ (pH 4.0) supplemented with 0.03% hydrogen peroxide. Color was allowed to develop for 10–15 minutes and the $A_{400}$ was read with a SpectraCount ELISA reader (Packard, Downers Grove, IL).

### Flow cytometric detection of cell-binding by biotinylated FNfn10 and FNfn10-3JCLI4

K562 cells ($10^5$) transfected with various integrins were resuspended in 5 ml FACS buffer (PBS, 0.5% BSA, 0.1% $NaN_3$), washed, and resuspended in FACS buffer containing either 0.4 μg/ml FNfn10 protein (wild-type or 3JCLI4) or 1 μg/ml LM609, prior to incubation at room temperature for 20 minutes. Cells were then washed with 5 ml FACS buffer, incubated in 1:50 streptavidin-APC (BD Pharmingen, San Diego, California) for 20 minutes and washed again with 5 ml FACS buffer, prior to detection of cell surface fluorescence using a FACSCalibur flow cytometer (Becton Dickinson, San Jose, California).

### Cell adhesion assays

Fibronectin and vitronectin-coated strips (Chemicon) were rehydrated 15 minutes in PBS. Inhibitor in IMDM/10% FBS was added to the bottom of the well, and $10^5$ cells/well in maintenance media were added to a final volume of 100 μl/ well. Cells were incubated two hours at 37 °C, 5% $CO_2$, washed three times with PBS at room temperature, and stained ten minutes with 0.2% (w/v) crystal violet, 10% (v/v) ethanol. Cells were then washed three times with PBS and solubilized with a 1:1 ratio of PBS:absolute ethanol for ten minutes with agitation. $A_{600}$ was measured using a SpectraCount ELISA reader (Packard).

### *In vitro* capillary tube formation

Quantimatrix (Chemicon, 40 μl) was added to wells of a 96-well plate (tube count determination) or 300 μl was added to a 24-well plate (total tube length determination) and solidified one hour at 37 °C. $1 \times 10^4$ (in total volume 50 μl, 96-well plate) or $4 \times 10^4$ (in total volume 100 μl, 24-well plate) SV-HCECs were added in maintenance media to the solidified matrix and incubated at 37 °C for three to five hours until capillary tubes formed in the presence of bFGF and the absence of inhibitor (positive control). To determine total number of tubes, wells were labeled numerically and tubes were counted by a blinded observer. To determine relative tube length, pictures were taken of the center of the well at 40× total magnification by a blinded observer, enlarged, and total tube length measured (total tube length of bFGF-treated cells without inhibitor = 1.0, other samples expressed as a relative total tube length). For purposes of classification, a completed capillary tube was counted if it stretched between two cell groups; cytoplasmic extensions were not counted.

## Acknowledgements

We thank Dr Scott Blystone for providing us with integrin-transfected K562 cells, Dr Angray Kang for the phage display vector, Drs Baek Kim, Jean Bidlack and Denise Hocking for helpful discussions and valuable input, and Lisa Rothgery for technical assistance. This work was supported by Department of Defense (DOD) grants to S.D. and S.K. (DAMD17-99-1-9361, DAMD17-01-1-0384, DAMD17-01-1-0385), and by NIH grant R29-GM55042 to S.K. J.R. is a trainee in the Medical Scientist Training Program funded by NIH grant T32 GM07356 and by T32 AI07362. The US Army Medical Research Acquistion Activity, 820 Chandler Street, Fort Detrick MD 21702-5014 is the awarding and administering acquistion office. This article does not necessarily reflect the position of the Government, and no official endorsement should be inferred.

## References

1. Wilson, D. R. & Finlay, B. B. (1998). Phage display: applications, innovations, and issues in phage and host biology. *Can. J. Microbiol.* **44**, 313–329.
2. Sidhu, S. S. (2000). Phage display in pharmaceutical biotechnology. *Curr. Opin. Biotechnol.* **11**, 610–616.
3. Lowman, H. B. (1997). Bacteriophage display and discovery of peptide leads for drug development. *Annu. Rev. Biophys. Biomol. Struct.* **26**, 401–424.
4. O'Neil, K. T., Hoess, R. H., Jackson, S. A., Ramachandran, N. S., Mousa, S. A. & DeGrado, W. F. (1992). Identification of novel peptide antagonists for GPIIb/IIIa from a conformationally constrained phage peptide library. *Proteins: Struct. Funct. Genet.* **14**, 509–515.
5. Main, A. L., Harvey, T. S., Baron, M., Boyd, J. & Campbell, I. D. (1992). The three-dimensional structure of the tenth type III module of fibronectin: an insight into RGD-mediated interactions. *Cell*, **71**, 671–678.
6. Carr, P. A., Erickson, H. P. & Palmer, A. G., III (1997). Backbone dynamics of homologous fibronectin type III cell adhesion domains from fibronectin and tenascin. *Structure*, **5**, 949–959.
7. Koide, A., Bailey, C. W., Huang, X. & Koide, S. (1998). The fibronectin type III domain as a scaffold for novel binding proteins. *J. Mol. Biol.* **284**, 1141–1151.
8. Weiss, J. M., Renkl, A. C., Maier, C. S., Kimmig, M., Liaw, L., Ahrens, T. *et al.* (2001). Osteopontin is involved in the initiation of cutaneous contact hypersensitivity by inducing Langerhans and dendritic cell migration to lymph nodes. *J. Expt. Med.* **194**, 1219–1229.
9. Horton, M. A. (1997). The alpha v beta 3 integrin "vitronectin receptor". *Int. J. Biochem. Cell. Biol.* **29**, 721–725.
10. Friedlander, M., Brooks, P. C., Shaffer, R. W., Kincaid, C. M., Varner, J. A. & Cheresh, D. A. (1995). Definition of two angiogenic pathways by distinct alpha v integrins. *Science*, **270**, 1500–1502.
11. Brooks, P. C., Stromblad, S., Sanders, L. C., von Schalscha, T. L., Aimes, R. T., Stetler-Stevenson, W. G. *et al.* (1996). Localization of matrix

metalloproteinase MMP-2 to the surface of invasive cells by interaction with integrin alpha v beta 3. *Cell*, **85**, 683–693.
12. Silletti, S., Kessler, T., Goldberg, J., Boger, D. L. & Cheresh, D. A. (2001). Disruption of matrix metalloproteinase 2 binding to integrin alpha vbeta 3 by an organic molecule inhibits angiogenesis and tumor growth *in vivo*. *Proc. Natl Acad. Sci. USA*, **98**, 119–124.
13. Kozlova, N. I., Morozevich, G. E., Chubukina, A. N. & Berman, A. E. (2001). Integrin alphavbeta3 promotes anchorage-dependent apoptosis in human intestinal carcinoma cells. *Oncogene*, **20**, 4710–4717.
14. Chatterjee, S., Matsumura, A., Schradermeier, J. & Gillespie, G. Y. (2000). Human malignant glioma therapy using anti-alpha(v)beta3 integrin agents. *J. Neurooncol.* **46**, 135–144.
15. Chatterjee, S., Brite, K. H. & Matsumura, A. (2001). Induction of apoptosis of integrin-expressing human prostate cancer cells by cyclic Arg-Gly-Asp peptides. *Clin. Cancer Res.* **7**, 3006–3011.
16. Brooks, P. C., Stromblad, S., Klemke, R., Visscher, D., Sarkar, F. H. & Cheresh, D. A. (1995). Antiintegrin alpha v beta 3 blocks human breast cancer growth and angiogenesis in human skin. *J. Clin. Invest.* **96**, 1815–1822.
17. Sipkins, D. A., Cheresh, D. A., Kazemi, M. R., Nevin, L. M., Bednarski, M. D. & Li, K. C. (1998). Detection of tumor angiogenesis *in vivo* by alphaVbeta3-targeted magnetic resonance imaging. *Nature Med.* **4**, 623–626.
18. Hufton, S. E., van Neer, N., van den Beuken, T., Desmet, J., Sablon, E. & Hoogenboom, H. R. (2000). Development and application of cytotoxic T lymphocyte-associated antigen 4 as a protein scaffold for the generation of novel binding ligands. *FEBS Letters*, **475**, 225–231.
19. Kumar, C. C., Nie, H., Rogers, C. P., Malkowski, M., Maxwell, E., Catino, J. J. & Armstrong, L. (1997). Biochemical characterization of the binding of echistatin to integrin alphavbeta3 receptor. *J. Pharmacol. Expt. Ther.* **283**, 843–853.
20. Blystone, S. D., Graham, I. L., Lindberg, F. P. & Brown, E. J. (1994). Integrin alpha v beta 3 differentially regulates adhesive and phagocytic functions of the fibronectin receptor alpha 5 beta 1. *J. Cell. Biol.* **127**, 1129–1137.
21. McLane, M. A., Vijay-Kumar, S., Marcinkiewicz, C., Calvete, J. J. & Niewiarowski, S. (1996). Importance of the structure of the RGD-containing loop in the disintegrins echistatin and eristostatin for recognition of alpha IIb beta 3 and alpha v beta 3 integrins. *FEBS Letters*, **391**, 139–143.
22. Hantgan, R. R., Endenburg, S. C., Cavero, I., Marguerie, G., Uzan, A., Sixma, J. J. & de Groot, P. G. (1992). Inhibition of platelet adhesion to fibrin(ogen) in flowing whole blood by Arg-Gly-Asp and fibrinogen gamma-chain carboxy terminal peptides. *Thromb. Haemost.* **68**, 694–700.
23. Scarborough, R. M., Rose, J. W., Naughton, M. A., Phillips, D. R., Nannizzi, L., Arfsten, A. *et al.* (1993). Characterization of the integrin specificities of disintegrins isolated from American pit viper venoms. *J. Biol. Chem.* **268**, 1058–1065.
24. Marcinkiewicz, C., Taooka, Y., Yokosaki, Y., Calvete, J. J., Marcinkiewicz, M. M., Lobb, R. R. *et al.* (2000). Inhibitory effects of MLDG-containing heterodimeric disintegrins reveal distinct structural requirements for interaction of the integrin alpha 9beta 1 with VCAM-1, tenascin-C, and osteopontin. *J. Biol. Chem.* **275**, 31930–31937.
25. Koivunen, E., Wang, B. & Ruoslahti, E. (1994). Isolation of a highly specific ligand for the alpha 5 beta 1 integrin from a phage display library. *J. Cell. Biol.* **124**, 373–380.
26. Oldenburg, K. R., Loganathan, D., Goldstein, I. J., Schultz, P. G. & Gallop, M. A. (1992). Peptide ligands for a sugar-binding protein isolated from a random peptide library. *Proc. Natl Acad. Sci. USA*, **89**, 5393–5397.
27. Smith, J. W., Tachias, K. & Madison, E. L. (1995). Protein loop grafting to construct a variant of tissue-type plasminogen activator that binds platelet integrin alpha IIb beta 3. *J. Biol. Chem.* **270**, 30486–30490.
28. Tani, P. H., Loftus, J. C. & Bowditch, R. D. (2002). *In vitro* selection of fibronectin gain-of-function mutations. *Biochem. J.* **365**, 287–294.
29. Altroff, H., van der Walle, C. F., Asselin, J., Fairless, R., Campbell, I. D. & Mardon, H. J. (2001). The eighth FIII domain of human fibronectin promotes integrin alpha5beta1 binding *via* stabilization of the ninth FIII domain. *J. Biol. Chem.* **276**, 38885–38892.
30. Pampori, N., Hato, T., Stupack, D. G., Aidoudi, S., Cheresh, D. A., Nemerow, G. R. & Shattil, S. J. (1999). Mechanisms and consequences of affinity modulation of integrin alpha(V)beta(3) detected with a novel patch-engineered monovalent ligand. *J. Biol. Chem.* **274**, 21609–21616.
31. Dickinson, C. D., Veerapandian, B., Dai, X.-P., Hamlin, R. C., Xuong, N.-H., Ruoslahti, E. & Ely, K. R. (1994). Crystal structure of the tenth type III cell adhesion module of human fibronectin. *J. Mol. Biol.* **236**, 1079–1092.
32. Xiong, J. P., Stehle, T., Diefenbach, B., Zhang, R., Dunker, R., Scott, D. L. *et al.* (2001). Crystal structure of the extracellular segment of integrin alpha Vbeta3. *Science*, **294**, 339–345.
33. Xiong, J. P., Stehle, T., Zhang, R., Joachimiak, A., Frech, M., Goodman, S. L. & Arnaout, M. A. (2002). Crystal structure of the extracellular segment of integrin alpha Vbeta3 in complex with an Arg-Gly-Asp ligand. *Science*, **296**, 151–155.
34. Suzuki, S., Huang, Z. S. & Tanihara, H. (1990). Cloning of an integrin beta subunit exhibiting high homology with integrin beta 3 subunit. *Proc. Natl Acad. Sci. USA*, **87**, 5354–5358.
35. Haisma, H. J., Grill, J., Curiel, D. T., Hoogeland, S., van Beusechem, V. W., Pinedo, H. M. & Gerritsen, W. R. (2000). Targeting of adenoviral vectors through a bispecific single-chain antibody. *Cancer Gene Ther.* **7**, 901–904.
36. Wickham, T. J., Haskard, D., Segal, D. & Kovesdi, I. (1997). Targeting endothelium for gene therapy *via* receptors up-regulated during angiogenesis and inflammation. *Cancer Immunol. Immunother.* **45**, 149–151.
37. Wickham, T. J., Segal, D. M., Roelvink, P. W., Carrion, M. E., Lizonova, A., Lee, G. M. & Kovesdi, I. (1996). Targeted adenovirus gene transfer to endothelial and smooth muscle cells by using bispecific antibodies. *J. Virol.* **70**, 6831–6838.
38. Hart, S. L. (1999). Integrin-mediated vectors for gene transfer and therapy. *Curr. Opin. Mol. Ther.* **1**, 197–203.
39. Kraulis, P. (1991). MOLSCRIPT: a program to produce both detailed and schematic plots of protein structures. *J. Appl. Crystallog.* **24**, 946–950.

40. Chappel, J. A., He, M. & Kang, A. S. (1998). Modulation of antibody display on M13 filamentous phage. *J. Immunol. Methods*, **221**, 25–34.
41. Kunkel, T. A. (1985). Rapid and efficient site-specific mutagenesis without phenotypic selection. *Proc. Natl Acad. Sci. USA*, **82**, 488–492.
42. Koivunen, E., Wang, B., Dickinson, C. D. & Ruoslahti, E. (1994). Peptides in cell adhesion research. *Methods Enzymol.* **245**, 346–369.

***Edited by I. Wilson***

*(Received 16 September 2002; received in revised form 30 December 2002; accepted 6 January 2003)*